Icarus 198 (2008) 37–56

Contents lists available at ScienceDirect

Icarus

www.elsevier.com/locate/icarus

Valley network-fed, open-basin lakes on Mars: Distribution and implications for Noachian surface and subsurface hydrology

Caleb I. Fassett, James W. Head III *

Department of Geological Sciences, Brown University, Providence, RI 02912, USA

ARTICLE INFO

Article history:
Received 27 March 2008
Revised 24 June 2008
Available online 8 August 2008

Keywords:
Mars, surface
Geological processes

ABSTRACT

A new catalog of 210 open-basin lakes (lakes with outlet valleys) fed by valley networks shows that they are widely distributed in the Noachian uplands of Mars. In order for an outlet valley to form, water must have ponded in the basin to at least the level of the outlet. We use this relationship and the present topography to directly estimate the minimum amount of water necessary to flood these basins in the past. The volumes derived for the largest lakes ($\sim 3 \times 10^4$ to $\sim 2 \times 10^5$ km^3) are comparable to the largest lakes and small seas on modern Earth, such as the Caspian Sea, Black Sea, and Lake Baikal. We determine a variety of other morphometric properties of these lakes and their catchments (lake area, mean depth, volume, shoreline development, outlet elevation, and watershed area). Most candidate lakes have volumes proportional to and commensurate with their watershed area, consistent with precipitation as their primary source. However, other lakes have volumes that are anomalously large relative to their watershed areas, implying that groundwater may have been important in their filling. Candidate groundwater-sourced lakes are generally concentrated in the Arabia Terra region but also include the Eridania basin [Irwin, R.P., Howard, A.D., Maxwell, T.A., 2004a. J. Geophys. Res. 109, doi: 10.1029/2004JE002287. E12009; Irwin, R.P., Watters, T.R., Howard, A.D. Zimbelman, J.R., 2004b. J. Geophys. Res. 109, doi: 10.1029/2004JE002248. E09011] and several lakes near the dichotomy boundary. This areal distribution is broadly consistent with where groundwater should have reached the surface as predicted by current models. Both surface runoff and groundwater flow appear to have been important sources for lakes and lake chains, suggesting a vertically integrated hydrological system, the absence of a global cryosphere, and direct communication between the surface and subsurface hydrosphere of early Mars.

1. Introduction

Analysis of Viking data revealed numerous candidate paleolakes on the surface of Mars (e.g., Goldspiel and Squyres, 1991; Cabrol and Grin, 1999, 2001). The criteria that these workers applied for recognizing lakes included a source of water (such as valley networks) and an enclosed, topographic low in which water would have ponded. To date, all of the global surveys assessing the presence of lake basins on Mars pre-date the acquisition of detailed topography by the Mars Orbiter Laser Altimeter (MOLA) (Smith et al., 1999) and High-Resolution Stereo Camera (HRSC) (Neukum et al., 2004). Thus, in this new analysis and survey, we utilize this new topographic information, as well as recently acquired high-resolution image data from Mars Global Surveyor, Mars Odyssey, Mars Express and Mars Reconnaissance Orbiter, to study the population of candidate lakes that once existed on the surface of Mars.

Both valley network (see, e.g., Pieri, 1980) and outflow channel (e.g., Baker and Milton, 1974) activity appear to have resulted in ponding of water and lake formation (De Hon, 1992; Cabrol and Grin, 1999, 2001). However, in this paper we limit our focus to lakes sourced by valley networks, which were active in the Noachian and persisted until approximately the Noachian–Hesperian boundary (Fassett and Head, 2008). Unlike outflow channels, which formed catastrophically and later in martian history, valley network-fed lakes are likely to have been longer-lived and closer to equilibrium with the surface environment when they formed. In this study, we direct our focus to candidate lakes characterized by clearly observed outlet valleys, which we thus interpret as having been were once open basins, in contrast to closed basins with valley sources but no outlet valleys.

The advantage of studying possible lakes where outlets are observed is that the outlets provide strong, direct evidence that lakes must have existed at these sites. In each instance, water needs to have ponded to great enough depth in the basin to form an outlet and breach the basin boundary. On this basis, we can then estimate a minimum volume of ponding in the basin using present topography. Thus, these open-basin lakes provide a constraint on the nature of the surface environment when they were active. These data in conjunction with information on input valley networks,

* Corresponding author.
E-mail address: James_Head_III@brown.edu (J.W. Head III).

0019-1035/$ – see front matter
doi:10.1016/j.icarus.2008.06.016

elevations, and relationship among connected lakes are useful in assessing the amount of water needed to fill the lakes, as well as the most likely sources of water to the basin (e.g., runoff and/or groundwater).

We organize this contribution into three parts. First, we discuss the methodology for identifying valley network-fed lakes and the criteria that we apply for their inclusion in our catalog. We then present our catalog of 210 open-basin lakes and describe their distribution, morphometry, and mapped connections to other lakes (where they form lake chains). Approximately 70% of these lakes are newly identified; where lakes have been previously mapped, our analysis adds their morphometric properties. We also discuss the geomorphology of the cataloged lake basins, focusing on their resurfacing history based on superposed impact crater populations. Finally, we explore the implications of this population of lakes for the atmospheric, surface, and subsurface environment of ancient Mars.

2. Methodology

Recent orbital missions to Mars have given us a wealth of information about the morphology and topography of its surface on local to global scales. For topographic information, we rely on a combination of MOLA gridded data at ~463 m/pixel (Smith et al., 1999) and high-quality HRSC stereo-derived digital terrain models (DTMs) at resolutions between 50 and 225 m/pixel (Scholten et al., 2005; Gwinner et al., 2007) (up through orbit 1526). The primary data we use for examining surface morphology are the Thermal Emission Imaging System (THEMIS) daytime infrared global image mosaics at 232 m/pixel (Christensen et al., 2004), but we also utilize THEMIS VIS, HRSC, and Viking MDIM2.1 to augment these data where higher resolution was necessary or where image gaps existed in THEMIS IR coverage. Daytime THEMIS IR images are excellent for recognizing and delineating subtle valley features, as the data emphasize relative solar illumination, highlighting topography such as valley walls. We integrate all our data in the ArcMap GIS environment to co-register images and allow intercomparison with topography.

Our current survey searched the surface of Mars from 90° S to 60° N latitude across all longitudes for candidate open basins, using image and topographic data together to avoid false positives. Specifically, we examine regions by manually flooding the topography over a narrow elevation range, searching for where valleys enter and leave basins. Our experience suggests that mapping lakes by automated flow routing and flooding of the surface of Mars based on topography alone (e.g., Kramer et al., 2003) can lead to the interpretation of lakes in areas with no evidence for source or outlet valleys, or on terrain such as Hesperian ridged plains that post-date the period of intense valley network formation and are likely volcanic. These regions thus lack clear evidence for having been water-filled basins.

We require two characteristics for a feature to be included in the catalog of open-basin lakes presented in Table 1. First, the observed feature must remain a basin on the basis of its present topography, so that if water were to enter the basin from either its catchment or from a groundwater source, it would pond. Second, there must be an outlet observed, suggesting that water flooded to sufficient depth to breach the basin boundary. Although lake basins can transition from open to closed behavior depending on climatic conditions, the incision of such an outlet is direct evidence that ponding of water and open basin behavior did occur at that location at some point in the past history of Mars.

3. Catalog of open-basin lakes

3.1. Locations and morphometry

A summary of the 210 cataloged open-basin lakes is given in Table 1, and their geographic distribution is shown in Fig. 1. An image of each lake is included in the supplementary material. Due to geological resurfacing events subsequent to the formation of valley networks and closed-basin lakes, the observed geographic distribution (Fig. 1) partly represents the original distribution and partly represents the overprinting effects of later geological history. For example, it is increasingly difficult to recognize valley-network drainage patterns at high latitude (south of ~30° S) due to the effects of recent mantling and terrain softening (Soderblom et al., 1973; Squyres and Carr, 1986; Kreslavsky and Head, 2000; Mustard et al., 2001). It is also challenging to recognize open basins in the broad regions of the highlands where younger plains units obscure the Noachian surface, for example in the broad Tharsis volcanic province (longitude 60° to 150° W) (see also Section 3.4 and discussion in Fassett and Head, 2008).

Morphometric parameters for the cataloged lakes (area, mean depth, volume, shoreline development and outlet elevation) are given in Table 1 along with their locations. These parameters are also graphically illustrated in Fig. 2. The distribution of the elevations of the 210 open-basin lakes is shown in Fig. 2a. Predictably, open-basin lakes are generally found at slightly lower elevations than valley networks as a whole. We expect this result because the formation of an open-basin lake would typically require a sufficiently large watershed to form a lake and overtop the basin. There also appears to be a weak inverse correlation between the volume of lakes and their elevation, as the largest quartile of lakes are ~300 m lower on average than the smallest of quartile lakes.

There is a very large range of sizes for the 210 lakes. Lake areas (Fig. 2b) span five orders of magnitude, from ~2 to ~500,000 km^2. Lake volumes (Fig. 2c) span seven orders of magnitude, from 0.02 to ~200,000 km^3. The largest open-basin lake that has been identified and meets the criteria of this study is the Eridania basin (Irwin et al., 2002, 2004a), which is larger than the modern Caspian Sea (volume of ~78,200 km^3). Another heavily degraded basin (#105) is found in the highlands with a volume of ~52,000 km^3, which connected to the extended network of Samara Vallis (see Fig. 3b). Three other basins with clear outlets (Fig. 4) have volumes of ~30,000 km^3: Antoniadi Crater (61° E, 21° N), Cassini Crater (36° E, 13° N), and Tikhonravov Crater (32° E, 24° N). Each of these lakes were once larger than Lake Baikal (~23,000 km^3), the largest modern terrestrial freshwater lake by volume. The potential hydrological role for these lakes is discussed in more detail below.

The areas and volumes for the open-basin lakes are strongly correlated (Fig. 2d). The best-fit power law has an exponent of 1.3, implying that lake volumes increase more quickly than lake areas. This requires that the mean depth, $\bar{d} = \frac{V}{A}$, also increases as lakes become larger in area. This area/volume relationship on Mars is consistent with what is commonly observed on Earth; similar exponents of 1.15 to 1.4 are common in terrestrial lake data sets (see, e.g., Ambrosetti and Barbanti, 2002; Schiefer and Klinkenberg, 2004; Håkanson, 2005). Mean depth (Fig. 2e) is commonly implicated as one of the most important morphometric parameters for the nature of lakes on Earth. This is because many studies have suggested that (all else being equal) lakes with more shallow water tend to have more nutrient cycling and biological productivity (see Wetzel, 2001, and references therein).

A final morphometric parameter of interest is the shoreline development index, defined as $D_L = \frac{L}{2\sqrt{\pi A}}$, where L is the length of the shoreline of the lake (Hutchinson, 1957). A perfectly circular basin would have $D_L = 1$; more irregular basins have a larger

Table 1
The catalog of 210 open-basin lakes on Mars compiled in this study. The reference is to the first paper that mentions a lake at this location

Lake #	Lon. (E)	Lat. (N)	Outlet elev.	Lake chain	Area (km^2)	Volume (km^3)	Reference
1	116.86	1.46	175	*a*	1.68E+02	8.41E+00	
2	151.78	−9.29	−670	*b*	2.37E+02	6.56E+00	Irwin et al. (2007)
3	166.75	−15.20	−1165	*c*	7.40E+01	2.18E+00	
4	−174.86	−14.63	580	*d*	9.43E+02	9.97E+01	Forsythe and Zimbleman (1995)
5	−161.57	−10.32	−1700	*e*	1.60E+02	1.50E+01	Cabrol and Grin (1999, 2001)
6	152.75	−11.53	540	*f*	4.45E+03	6.16E+02	Irwin et al. (2007)
7	157.12	−12.44	−280	*f*	2.90E+02	2.87E+01	
8	42.19	18.25	−280	*n*	6.57E+03	4.89E+02	
9	59.68	27.47	250	*h*	3.60E+03	4.81E+02	
10	60.94	21.10	500	*h*	9.58E+04	3.10E+04	
11	63.02	26.57	440	*h*	1.13E+04	1.08E+04	
12	100.97	−1.31	685	*i*	1.65E+02	5.74E+00	
13	102.02	0.92	−650	*i*	6.61E+02	1.29E+01	
14	102.36	2.42	−850	*i*	6.83E+02	3.13E+01	
15	−169.20	−18.30	940		2.38E+02	2.76E+01	Cabrol and Grin (1999, 2001)
16	−12.32	−21.67	−1075	*w*	1.12E+04	1.55E+03	Goldspiel and Squyres (1991)
17	−8.59	25.57	−2350		1.90E+03	1.14E+02	
18	−7.21	−8.84	−1400	m_2	2.48E+04	8.25E+03	
19	2.77	−10.63	−760	*m*	1.24E+04	4.25E+03	
20	60.11	31.33	−975		6.13E+02	1.60E+02	
21	63.03	30.85	−550		7.53E+03	4.67E+03	
22	78.43	−3.73	145		3.15E+03	2.72E+02	
23	84.96	−2.42	1325	*o*	1.79E+03	1.05E+02	
24	84.96	−4.46	1725	*o*	1.50E+03	8.36E+01	
25	89.71	−0.09	−185		9.55E+02	1.55E+02	Cabrol and Grin (1999, 2001)
26	90.01	−4.57	860		1.72E+02	1.57E+01	Cabrol and Grin (1999, 2001)
27	108.19	−2.84	−55	*k*	2.15E+02	1.31E+01	Cabrol and Grin (1999, 2001)
28	109.22	−4.00	110	*k*	4.56E+03	1.23E+03	
29	110.86	−2.71	−675		9.77E+02	5.74E+01	Cabrol and Grin (1999, 2001)
30	144.06	−11.74	390	*x*	2.60E+02	1.50E+01	Cabrol and Grin (1999, 2001)
31	154.52	−10.77	200		1.93E+02	1.87E+01	
32	−23.53	−23.12	−890	*j*	1.38E+03	1.01E+02	
33	−5.32	−5.51	−1310	m_2	3.87E+02	3.65E+01	Cabrol and Grin (1999, 2001)
34	102.25	−3.42	975		9.22E+02	4.12E+01	
35	3.88	−27.90	1210	*m*	1.34E+04	6.24E+02	
36	31.05	13.18	−525	*n*	1.01E+03	3.42E+01	Irwin et al. (2005a)
37	31.58	10.02	−340	*n*	7.91E+03	3.38E+02	Irwin et al. (2005a)
38	35.46	1.30	445	*n*	6.99E+02	4.93E+01	Cabrol and Grin (1999, 2001)
39	41.98	−6.37	1440	*n*	6.89E+02	5.03E+01	Cabrol and Grin (1999, 2001)
40	25.57	29.91	−1850	*n*	2.09E+03	5.36E+02	McGill (2002)
41	31.72	24.39	−1135	*n*	8.27E+04	3.02E+04	
42	36.40	20.04	−950	*n*	1.32E+02	9.24E+00	
43	35.08	18.99	−1120	*n*	2.90E+02	1.38E+01	
44	33.57	16.72	−1200	*n*	1.08E+04	5.26E+02	
45	77.70	18.38	−2390		1.22E+03	2.37E+02	Fassett and Head (2005)
46	127.20	−10.32	1830	*q*	4.03E+01	1.59E+00	
47	128.01	−10.37	1760	*q*	3.02E+01	6.06E−01	
48	131.05	−7.35	1090	*q*	1.07E+02	5.47E+00	
49	127.05	−4.58	1220		6.50E+02	6.98E+01	Irwin et al. (2007)
50	175.39	−14.40	−1700	*s*	1.45E+04	2.41E+03	Cabrol and Grin (1999, 2001)
51	176.56	−30.12	950	*s*	4.93E+05	2.13E+05	Irwin et al. (2002)
52	−48.00	8.54	−1720	*dd*	1.76E+01	4.40E−01	Harrison and Grimm (2005)
53	17.06	33.80	−2600	*n*	3.68E+03	1.98E+03	Cabrol and Grin (1999, 2001)
54	18.19	34.61	−2225	*n*	1.13E+02	2.37E+00	Cabrol and Grin (1999, 2001)
55	18.04	34.17	−2300	*n*	3.57E+02	1.85E+01	Cabrol and Grin (1999, 2001)
56	−155.77	−12.07	−320		3.67E+02	1.31E+01	
57	−158.65	−15.45	200	*aa*	2.10E+02	8.01E+00	
58	26.65	27.92	−1755	*n*	8.19E+01	9.56E+00	McGill (2002)
59	59.62	−20.31	−240	*u*	1.43E+03	1.01E+02	Lahtela et al. (2005)
60	60.63	−20.99	−300	*u*	1.60E+03	9.58E+01	Lahtela et al. (2005)
61	−102.96	−38.91	3410	*t*	3.77E+01	9.63E+00	
62	−91.82	−41.86	5065		2.84E+01	7.81E−01	
63	125.18	−0.81	−30		8.62E+01	2.01E+00	Irwin et al. (2007)
64	126.62	−1.60	80		1.28E+02	3.72E+00	Irwin et al. (2007)
65	−12.27	−23.44	−760	*w*	3.52E+02	4.49E+01	Irwin et al. (2007)
66	−6.32	−19.36	−290	*l*	3.50E+02	1.54E+02	
67	4.05	−21.49	590	*m*	4.13E+02	8.52E+01	
68	151.35	−10.28	210	*b*	1.60E+02	5.23E+00	Irwin et al. (2007)
69	61.43	27.33	55	*h*	8.52E+01	7.05E+00	
70	135.38	−6.91	−400	*z*	1.53E+03	2.48E+02	
71	136.47	−6.72	−690	*z*	4.28E+01	4.30E+00	
72	134.92	−9.45	685	*z*	1.31E+03	2.52E+02	Cabrol and Grin (1999, 2001)
73	134.07	−11.22	1050	*z*	9.11E+02	9.00E+01	
74	−167.18	−9.54	−1395	*r*	1.51E+02	1.26E+01	
75	−165.61	−10.22	−1450	*r*	4.52E+03	1.16E+03	Cabrol and Grin (1999, 2001)

(*continued on next page*)

Table 1 (*continued*)

Lake #	Lon. (E)	Lat. (N)	Outlet elev.	Lake chain	Area (km^2)	Volume (km^3)	Reference
76	−162.87	−5.88	−2560	*e*	3.73E+01	2.15E+00	
77	134.49	−23.21	1770		9.27E+02	8.50E+01	
78	123.25	0.07	195		3.02E+01	1.65E+00	
79	161.08	−14.00	−895	*g*	5.00E+01	4.25E+00	
80	159.46	−22.78	680	*v*	2.74E+02	9.70E+00	
81	−1.73	−4.23	−1455		6.72E+02	9.52E+01	
82	62.17	−2.56	2125		1.71E+03	4.35E+01	
83	−18.29	−26.87	−380	*j*	1.29E+03	6.01E+01	
84	87.00	−20.47	965		5.40E+02	5.69E+01	
85	96.52	−13.32	1975		1.08E+03	5.35E+01	
86	56.22	−21.58	515	*cc*	2.00E+02	3.73E+00	
87	94.29	−6.29	930		1.08E+02	6.85E+00	
88	149.44	−8.68	−495		8.11E+01	1.01E+00	
89	167.28	−16.01	−1080	*c*	1.08E+02	4.79E+00	Cabrol and Grin (1999, 2001)
90	170.73	−19.98	−85	*ee*	4.25E+02	1.34E+01	Cabrol and Grin (1999, 2001)
91	171.33	−17.44	−620	*ee*	1.43E+03	5.23E+02	Cabrol and Grin (1999, 2001)
92	171.28	−18.21	−500	*ee*	1.78E+02	7.79E+00	
93	16.44	−12.82	1110	*mm*	8.11E+01	4.05E+00	Cabrol and Grin (1999, 2001)
94	−13.68	−53.37	615	*ll*	2.86E+03	3.68E+02	
95	−20.51	−22.45	−935	*j*	4.87E+02	8.49E+00	Goldspiel and Squyres (1991)
96	147.24	−29.81	1050	*hh*	9.36E+01	3.99E+00	
97	147.58	−29.85	990	*hh*	9.45E+01	2.63E+00	
98	78.13	−19.71	355	*ii*	1.05E+02	4.44E+00	
99	77.62	−18.85	575	*ii*	2.72E+02	1.48E+01	
100	71.01	−23.42	−2150		7.71E+01	1.29E+00	
101	76.48	−23.09	−685	*kk*	2.07E+00	2.32E−02	
102	75.60	−23.20	−870	*kk*	2.92E+03	1.46E+02	
103	75.91	−22.10	325	*kk*	2.21E+01	6.20E−01	
104	78.17	−20.07	350	*ii*	6.82E+01	2.50E+00	
105	−24.35	−41.10	1260	*j*	2.22E+05	5.23E+04	
106	−22.31	−63.24	670	*nn*	1.34E+03	9.26E+01	Cabrol and Grin (1999, 2001)
107	−19.96	−62.90	905	*nn*	2.46E+02	4.49E+01	Cabrol and Grin (1999, 2001)
108	−24.35	−55.22	−30	*ll*	4.81E+02	1.94E+01	
109	−24.39	−54.69	−30	*ll*	5.48E+02	7.68E+00	
110	−18.98	−52.89	390	*ll*	7.74E+03	2.95E+02	
111	11.70	−12.71	370	*mm*	2.84E+02	2.20E+01	
112	19.52	13.20	−1250		1.99E+02	4.88E+01	
113	−32.41	−59.68	−765	*nn*	1.26E+03	4.75E+02	
114	−9.79	−37.20	1165	*j*	5.76E+02	1.06E+01	
115	74.42	26.76	−200		2.47E+03	9.16E+02	
116	93.40	−3.84	1000		7.38E+01	3.93E+00	
117	26.18	28.70	−1800	*n*	1.08E+02	3.23E+00	
118	68.86	32.05	−880	*oo*	1.00E+03	2.30E+02	
119	68.58	29.33	50	*oo*	1.83E+03	9.43E+02	
120	68.04	30.29	−190	*oo*	6.79E+02	3.08E+02	
121	−174.46	−16.10	1140	*d*	3.59E+02	1.53E+01	
122	−31.70	−60.14	−690	*nn*	2.92E+02	4.10E+01	
123	−21.67	−20.42	−1360	*j*	5.97E+02	2.70E+01	
124	33.08	26.73	−710	*n*	1.35E+02	2.53E+00	
125	36.11	18.88	−1000	*n*	1.27E+03	2.80E+02	
126	57.62	−21.65	60	*cc*	1.01E+03	1.11E+02	
127	115.88	2.22	310	*a*	1.02E+03	4.15E+01	
128	80.91	−33.83	−5375		3.81E+02	3.51E+01	Cabrol and Grin (1999, 2001)
129	−4.87	−11.92	−1400	m_2	3.02E+02	1.02E+01	
130	−177.87	−11.99	−950		1.88E+02	4.50E+01	
131	22.25	−5.02	1800	*pp*	9.99E+01	1.80E+00	
132	24.69	−17.98	1900		7.08E+02	1.01E+02	
133	18.96	30.95	−2325	*n*	2.67E+02	2.18E+01	Cabrol and Grin (1999, 2001)
134	161.26	−13.43	−1185	*g*	5.08E+02	2.65E+01	
135	−103.31	−39.19	2780	*t*	3.38E+02	1.59E+02	Mangold and Ansan (2006)
136	−100.69	−38.57	3370	*t*	7.79E+03	1.44E+03	Mangold and Ansan (2006)
137	85.38	−26.11	−890		4.18E+01	1.56E+00	
138	−6.34	−19.05	−305	*l*	1.99E+01	6.57E−01	Irwin et al. (2005a)
139	28.76	−0.03	950		2.31E+03	4.46E+02	Cabrol and Grin (1999, 2001)
140	38.08	−0.38	715	*n*	3.02E+02	9.87E+00	Cabrol and Grin (1999, 2001)
141	−22.18	−15.03	−1800	*j*	1.00E+02	1.09E+01	Cabrol and Grin (1999, 2001)
142	−150.98	−48.54	2095		5.43E+01	1.42E+00	
143	14.66	−53.90	1310		6.68E+02	2.75E+01	
144	−11.46	−36.28	1035	*j*	1.52E+03	2.56E+01	
145	−14.02	−31.50	805	*j*	2.97E+02	5.89E+00	
146	−23.58	−22.28	−1025	*j*	1.56E+02	9.86E+00	
147	−4.04	−26.48	575	*l*	4.48E+01	1.95E+00	
148	−11.15	−26.81	500	*w*	6.00E+02	8.71E+00	
149	41.11	−10.00	2500	*n*	2.56E+02	1.29E+01	
150	41.54	−9.01	2275	*n*	3.79E+02	2.69E+01	
151	66.65	26.43	70	*y*	2.60E+03	2.50E+02	

Table 1 (*continued*)

Lake #	Lon. (E)	Lat. (N)	Outlet elev.	Lake chain	Area (km^2)	Volume (km^3)	Reference
152	67.22	27.72	20	*y*	7.42E+02	1.96E+02	
153	86.64	3.06	−2975		4.25E+01	2.86E+00	
154	174.88	−18.66	150		2.02E+02	8.22E+00	
155	−159.65	−11.63	−935	*aa*	3.64E+02	2.08E+01	
156	−159.75	−11.24	−975	*aa*	2.28E+02	1.13E+01	
157	−54.89	−40.41	1225		2.16E+02	6.36E+00	
158	−58.38	−45.16	500		3.52E+03	6.16E+02	
159	−45.66	−37.48	−850	*bb*	1.08E+02	3.72E+00	
160	−45.17	−36.73	−160	*bb*	1.46E+02	4.14E+00	
161	−44.62	−36.24	−45	*bb*	8.17E+01	1.85E+00	
162	−44.63	−35.70	155	*bb*	1.75E+02	3.72E+00	
163	−45.29	−37.44	−820		8.19E+01	2.46E+00	
164	15.68	−11.16	1250	*mm*	2.61E+02	1.59E+01	
165	39.08	20.78	−620	*n*	4.25E+03	2.25E+03	
166	24.35	−6.44	2020		3.42E+02	1.11E+01	
167	102.77	−1.93	680		1.44E+02	6.82E+00	
168	−46.18	9.63	−2200	*dd*	5.55E+01	2.15E+01	
169	139.72	−8.64	995		1.37E+02	4.18E+00	Irwin et al. (2007)
170	142.36	−10.26	530		3.85E+02	6.14E+01	Irwin et al. (2007)
171	−5.25	−21.26	−60	*l*	3.38E+04	4.84E+03	Irwin et al. (2007)
172	131.84	−10.05	1730		1.20E+02	1.78E+00	
173	131.44	−10.54	2250		3.75E+01	8.03E−01	
174	132.47	−10.73	1685		7.83E+01	1.12E+00	
175	132.51	−22.03	1935		1.43E+02	7.04E+00	
176	142.05	−27.06	1850		5.91E+01	1.16E+00	
177	141.34	−26.86	2125		8.13E+01	4.46E+00	
178	37.10	27.33	−1265		9.47E+02	3.89E+01	
179	32.30	20.57	−815	*n*	4.93E+02	1.95E+01	
180	179.15	−34.02	1490		1.89E+02	6.38E+00	
181	46.56	−5.74	2030	*n*	3.56E+02	1.31E+01	
182	57.31	−5.59	2267		1.88E+01	1.44E−01	
183	43.76	−5.13	1335	*n*	2.97E+02	1.51E+01	
184	33.60	−2.76	1250	*n*	3.86E+02	2.74E+01	
185	45.51	2.16	1510		1.07E+02	4.89E+00	
186	42.91	0.52	1130	*n*	6.58E+01	1.82E+00	
187	42.99	−7.16	2010	*n*	6.17E+02	5.95E+01	
188	36.12	13.12	−650	*n*	6.19E+04	3.23E+04	
189	38.37	14.88	230	*n*	2.13E+02	5.40E+00	
190	−18.15	−16.51	−1290	*w*	8.29E+02	4.40E+01	
191	6.05	−24.92	1585	*m*	1.23E+02	2.29E+00	
192	6.71	−23.45	1120	*m*	1.43E+03	5.10E+02	
193	21.96	−4.49	1460	*pp*	2.02E+02	7.59E+00	
194	86.92	2.96	−2370		1.17E+01	1.73E−01	
195	83.20	3.51	−2695		2.65E+01	7.03E−01	
196	91.26	0.61	−240		4.88E+01	2.13E+00	
197	89.84	3.25	−2850		5.45E+02	5.82E+01	
198	94.61	5.81	−2695		6.36E+01	1.96E+00	
199	158.54	−22.89	800		2.61E+03	2.33E+03	
200	102.49	1.08	−690		5.27E+01	1.41E+00	
201	112.13	−2.39	−575		5.02E+02	3.88E+01	
202	39.74	5.16	940		4.12E+03	2.59E+02	
203	126.63	−3.77	960		4.29E+00	2.24E−02	
204	−23.19	−41.24	160		1.10E+02	4.79E−01	
205	25.51	−31.11	1945		7.40E+01	3.13E+00	
206	21.21	−30.59	1840		4.81E+01	2.78E+00	
207	25.25	−32.75	2435		1.68E+02	5.08E+01	
208	160.98	−17.11	−280	*g*	5.47E+02	5.11E+01	
209	101.58	−0.90	1060	*i*	7.90E+01	2.23E+00	
210	−4.52	−5.08	−1415		2.51E+01	7.52E−01	

shoreline development index. Lakes with larger shoreline development indices are likely to be more affected by littoral zone or shoreline processes, such as wave and current modification, than more circular lakes of equal area (Hutchinson, 1957). In this study, shoreline length was measured using the contour defined by the basin outlet. The majority of basins have comparatively small shoreline development indices (Fig. 2f), likely due to the fact that the vast majority of the open-basin lakes that we catalog formed in pre-existing impact craters. Open-basin lakes with comparatively high development indices (the nine lakes with $D_L > 3$) formed in a variety of topographic settings, including places where multiple deep basins were simultaneously flooded (e.g., Eridania) and where broad regions of low topographic relief were flooded, leading to irregular shorelines and unusually low mean depths for their size (e.g., #37).

3.2. Lake chains

There has been recognition in the last ten years that some basins on Mars are part of chains of lakes (e.g., Cabrol and Grin, 1999; Irwin et al., 2005a). However, one of the most striking observations of our survey is that the majority of the open-basin lakes on Mars formed as part of connected lake-chain systems. Of the 210 open-basin lakes that we catalog in Table 1, 138 (66%) are part of an integrated lake system (connected by valley networks to other lakes). By definition, outlet valleys of open-basin lakes cross

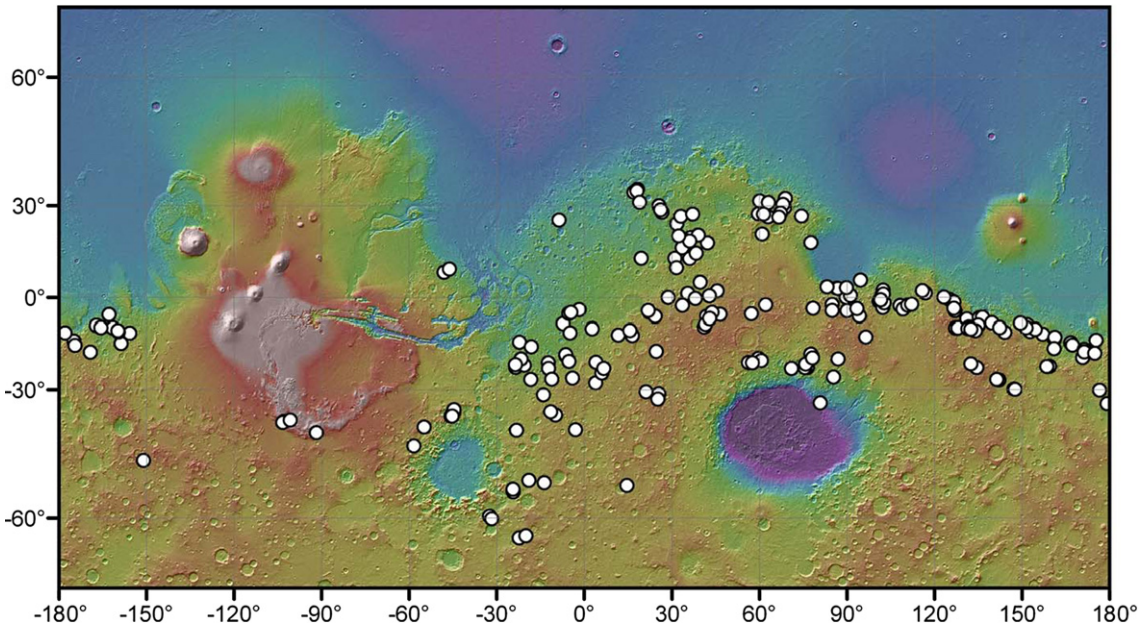

Fig. 1. The locations of the 210 open-basin lakes compiled in this study. The geographic distribution is a complex combination of initial lake location as well as subsequent burial and obliteration.

local drainage divides. Because of this, these lake-chain systems were significant pathways for integration of the surface hydrology of early Mars. The drainage paths which are established by the valley–lakes chain systems we observe are broadly consistent with drainage basins defined at the largest scale (e.g., Banerdt and Vidal, 2001).

The frequency distribution of the lengths of lake chains (Fig. 5) shows that most of the lake-chain systems are continuous over length scales of 200–600 km, but a few are longer than 1000 km (Fig. 3). For example, the Naktong/Scamander/Mamers Valles lake-chain system (Irwin et al., 2005a) is ~4500 km long, with at least 30 separate basins contributing to its flow (Fig. 3a). The length and watershed area ($A_w \sim 2.4 \times 10^6$ km^2) of this valley/lake-chain system is comparable to the largest terrestrial systems such as the Missouri–Mississippi River drainage (~6000 km long; $A_w \sim 3 \times 10^6$ km^2). However, the Naktong/Scamander/Mamers valley system has numerous intra-valley lakes (Fig. 3a), unlike large terrestrial drainages. This is likely a result of the immaturity of the martian landscape compared to that of Earth.

Other lake chains longer than 1000 km include the Samara/Himera Vallis lake-chain system, with a length of ~1800 km and at least nine basins contributing to its flow (Fig. 3b), including a very large, degraded basin at its head. Near the Samara/Himera system, the ~1100 km long Parana/Loire system had at least four connected basins (Fig. 3c). A final example is a long valley–lake system at 3.5° E (22° S to 10° S) (Fig. 3d), which enters Madler crater and was fed by at least five basins. It had an end-to-end length of at least 1200 km and likely up to ~1800 km; we infer a connection to the west to the crater at 7° W, 9° S (Fig. 3d, dashed line). However, the region where this connection likely once existed has been heavily obscured by resurfacing.

Many of the longest integrated lake-chain systems (Fig. 3) on Mars are found in the region from 40° W to 60° E longitude, and they are especially concentrated in the region of Margaritifer Sinus (see Grant and Parker, 2002). There are two possible explanations for this concentration, which are not mutually exclusive. First, this region might have been climatologically wetter than others, supplying substantially more water flux, as suggested by Irwin et al. (2007). Secondly, broad patterns of groundwater circulation might have played an important role in preferentially supplying water to this region (e.g., Andrews-Hanna et al., 2007, 2008).

3.3. Watershed delineation

A very important part of understanding lakes and lake-chain systems is determining the area of the watershed that contributed to the lake. We estimate the contributing watershed area (A_w) of 73 of the cataloged basins (Table 2), a subsample excluding (1) basins that had other volumetrically important basins as a contributing source (such as those fed in lake chains discussed above), and (2) lakes that appear to have experienced major resurfacing in their watershed that complicates watershed definition.

After measuring the contributing catchment area, we calculated the lake volume/watershed area ratio (V/A_w) which has dimensions of depth. From the water balance equation, this ratio can be expressed as:

$$V/A_w = \tau\big((P - E) + (G_i - G_o)\big), \quad (1)$$

where precipitation (P) (input to the lake either directly or as runoff), evaporation (E), and the groundwater flow balance (G_i, groundwater inflow; G_o, groundwater infiltration) are expressed per unit area of the watershed, and τ is the basin-filling timescale. This ratio is thus a measure of the time-integrated sources of water to a lake in excess of infiltration/evaporation. For the lake to fill and overflow, precipitation and groundwater inputs must have exceeded the loss mechanisms in each open basin over the time period τ that it took to fill the lake.

The majority (60/73) of the lakes for which we measured V/A_w have ratios of <15 m (Fig. 6A). The best-fit power law describing the relationship of volume and watershed area for these lakes is $V = 0.0018(A_w^{1.006})$ ($R^2 = 0.65$). The near-unity exponent for this power-law fit implies that the volume of these open-basin lakes was directly proportional to their contributing watershed area. This is consistent with what we expect if the lakes were sourced predominantly by precipitation to their catchments, as watershed area multiplied by precipitation depth is a direct measure of the precipitation-controlled source terms to the lakes (direct precipitation, runoff, and locally recharged groundwater).

Some lakes (13/73) are clear outliers in the distribution of the ratio of volume to watershed area, with V/A_w ratios up to two

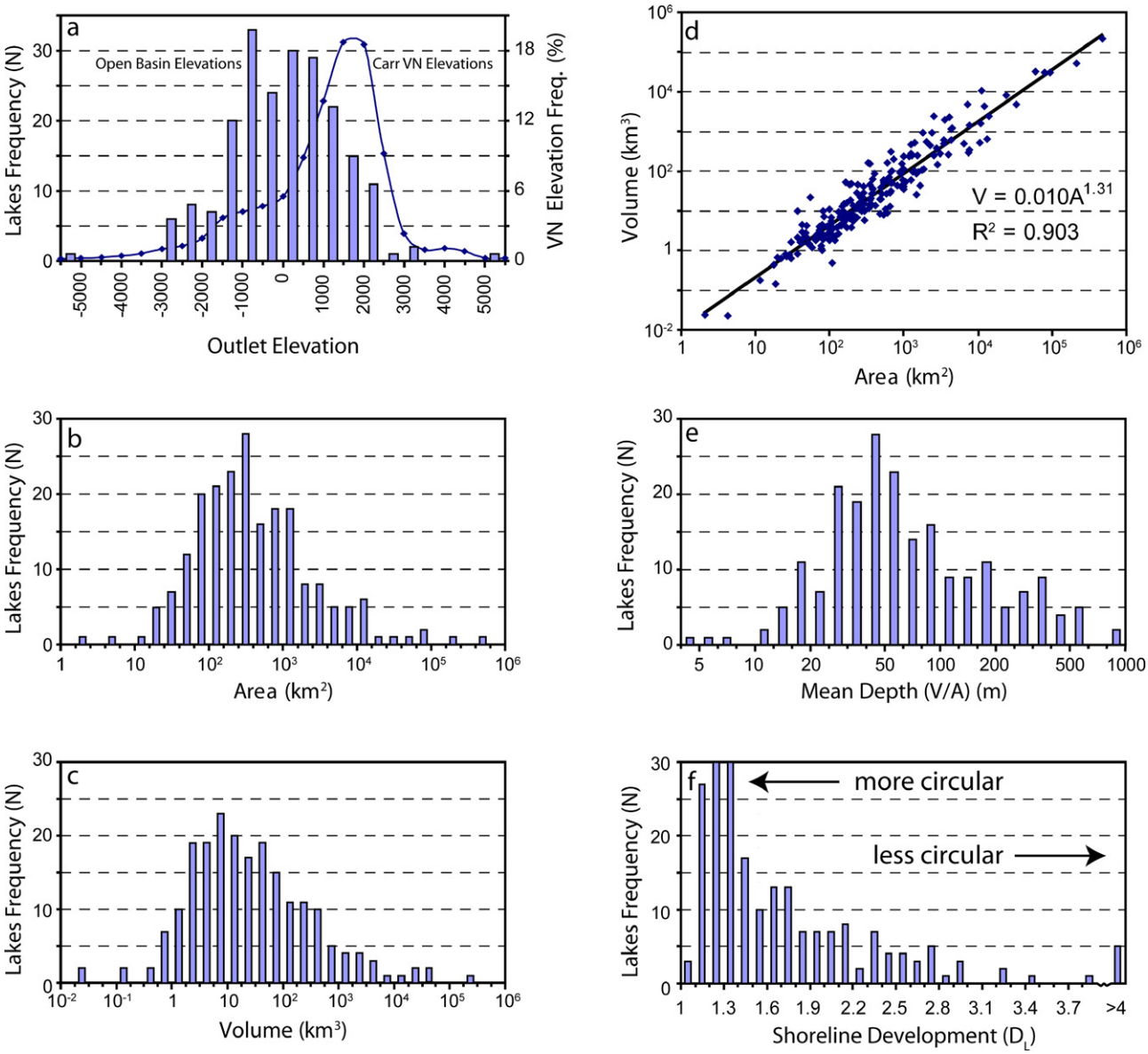

Fig. 2. (a) MOLA elevations of outlets of the catalogued open-basin lakes and of valley networks. The valley network elevations are derived from mapping by Carr (1996). The population of observed lakes falls at a somewhat lower elevation than do the valley networks as a whole. (b) Frequency distribution of area for the catalogued lakes. (c) Frequency distribution of volume for the catalogued lakes. (d) Log–log plot of volume vs area for the catalogued lake population. (e) Frequency distribution of mean depth for the catalogued lakes. (f) Frequency distribution of shoreline development index for the catalogued lakes.

orders of magnitude above the median (Fig. 6A; Table 2). Filling these high V/A_w basins requires that their water sources (direct precipitation, runoff, groundwater input) were more important than their loss mechanisms (evaporation, groundwater infiltration) compared to typical lakes we measured. One possibility is that the presence of such areally significant lakes altered the local evaporation–precipitation cycle via lake-atmosphere feedback, as is important for large terrestrial lakes (e.g., Hostetler et al., 1994). However, other characteristics of these lakes and their drainage basins are likely inconsistent with this explanation: first, many lakes that are V/A_w anomalies commonly have poorly integrated source drainage basins, which is why they have minimal drainage area relative to volume. Second, the source valleys draining their watersheds are usually relatively small, and appear unlikely to have transported excess precipitation into the basin compared to other open-basin lake feeders.

An alternative possible explanation for changing the water balance for these basins with $V/A_w \gg 15$ (see Eq. (1)) is if groundwater was an important contributor to their filling. In principle, if this groundwater was only recharged on the local watershed and reached the lake through a local flow system, the volume that basins fill should have remained approximately proportional to watershed area. Therefore, for the V/A_w ratio to rise as a result of groundwater flow, this groundwater cannot be simply recharged locally and must be transported into the catchment from another basin. Because surface drainage divides and watersheds do not control the patterns of long-wavelength groundwater flow (e.g., Winter, 1999; Fetter, 2001; see also Clifford, 1993), such a regional source is very plausible. Lakes exist in a variety of geological settings on Earth where regional-scale groundwater flow is an important input source (e.g., Winter, 1999). Although the existence of very large lakes may have led to precipitation–evaporation feedback effects once large lakes existed, groundwater input to these lakes would help explain how these particular basins ended up filling sufficiently to form outlet valleys.

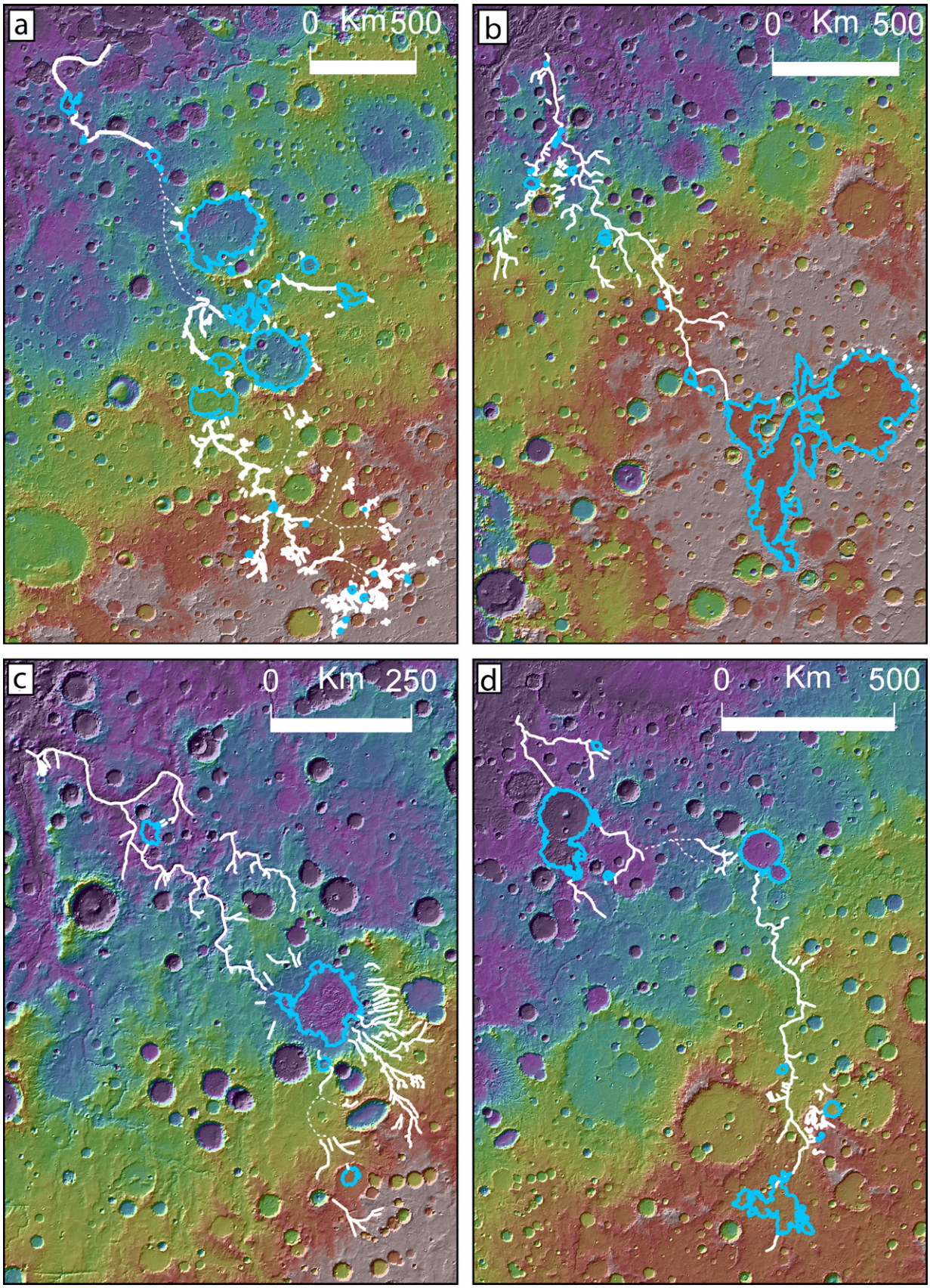

Fig. 3. Examples of the longest lake chains in our catalog (excluding Ma'adim Vallis; see Irwin et al., 2002). (a) The Naktong–Scamander–Mamers lake-chain system (see Irwin et al., 2005a) (*n* in Table 1) (~4500 km long). The regions with the dashed lines were almost certainly interconnected based on present topographic divides, but these areas have been heavily resurfaced, and no clear lakes or valleys are present. (b) The Samara Vallis lake-chain system (*j* in Table 1) (~1800 km long). (c) The Parana–Loire valley network and lake-chain system (*w* in Table 1) (~1100 km long). (d) An unnamed valley–lake system (*m* in Table 1), flowing north into Mädler crater (> ~1200 km long). The dashed line from Mädler to the west connects to another lake-chain system (m_2 in Table 1); this connection has to be inferred because of resurfacing.

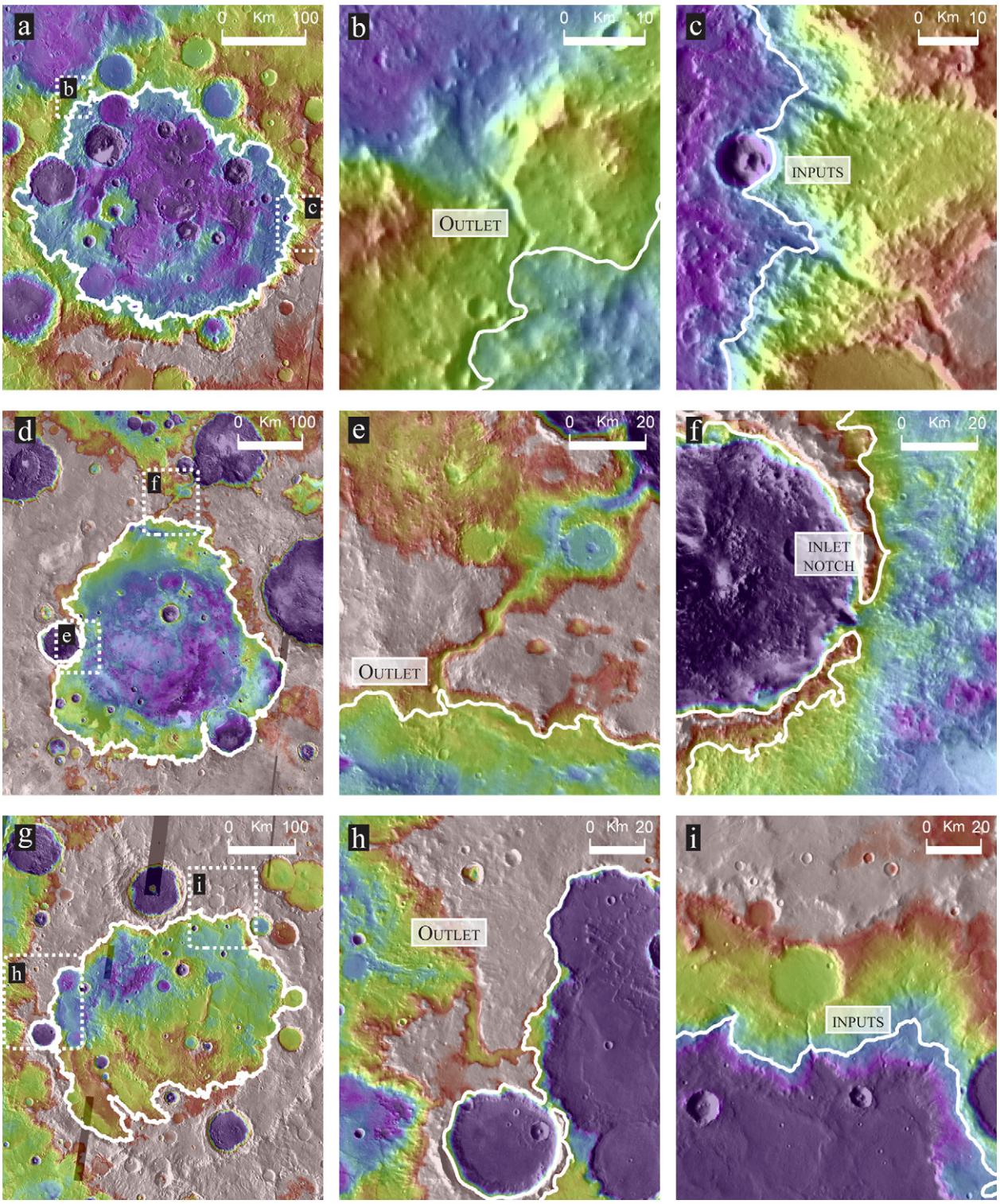

Fig. 4. Three of the largest open basins on Mars ($V > 30{,}000$ km^3, $V/A_w > 15$, see Table 2). (a) Tikhonravov crater ($D \sim 370$ km). (b) Rim breach on the NW rim of Tikhonravov; the outlet feeds into another breached basin that connects to the Naktong/Scamander drainage system. (c) Valleys on the Tikhonravov basin rim, terminating at approximately the breach contour (−650 m). (d) Antoniadi crater ($D \sim 410$ km) NW of Syrtis Major. (e) Rim breach of Antoniadi to the north, sourcing Auqakuh Vallis through a series of other breached basins. (f) A notch in the west rim of Antoniadi, connecting it to a fresher deep crater that was also filled. (g) Cassini crater ($D \sim 430$ km). (h) Rim breach of Cassini, in its western rim, connecting to Naktong/Scamander (as does a). (i) Valleys terminating near the breach contour (−1135); the small valley in the center of the frame is an outlet breach for a small open basin.

The locations of basins that are candidates for being sourced significantly by groundwater are shown in Fig. 7a. The four largest open-basin lakes in our catalog by volume for which we have watershed measurements are all substantial V/A_w anomalies ($V/A_w > 100$ m) (see Section 3): Eridania (Irwin et al., 2002, 2004a, 2004b), Tikhonravov (Figs. 4a–4c), Antoniadi (Figs. 4d–4f) and Cassini (Figs. 4g–4i).

If the hypothesis is correct that the open-basin lakes that are anomalous in V/A_w were significantly fed by groundwater, it provides direct information about the nature of the coupling of the

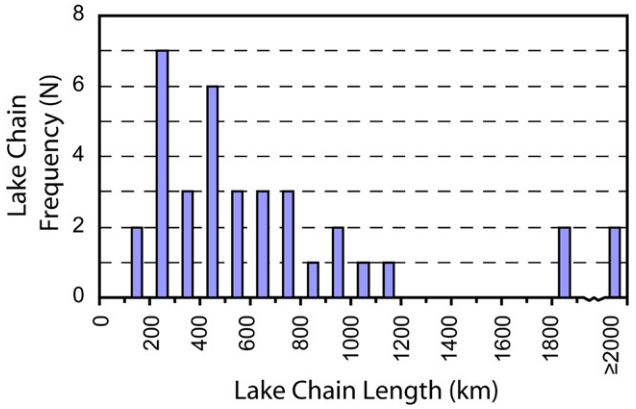

Fig. 5. Frequency distribution of the end-to-end length of lake chains on Mars mapped in this study. Most lake chains are less than 1000 km long, but a few are much longer (see Fig. 3).

surface and subsurface hydrology of Noachian Mars and helps to identify where groundwater was reaching the surface. Such independent observations can help to constrain models of large-scale groundwater flow and release (e.g., Clifford, 1993; Andrews-Hanna et al., 2007, 2008).

Numerical models exploring large-scale patterns of groundwater flow on Mars have recently been constructed by Andrews-Hanna et al. (2007, 2008). These models solve the Boussinesq equation for patterns of groundwater flow forced by topography and a precipitation/evaporation cycle with the following assumptions: First, maximum precipitation is assumed to be focused at the equator, with a cosine distribution of precipitation extending from 45° S to 45° N. The assumption that precipitation is focused in this area around the equator concentrates groundwater recharge in this region as well. Second, all water that reaches the surface from groundwater is assumed to evaporate upon reaching the surface, rather than running off and/or concentrating in lakes. The globally integrated evaporative flux is then redistributed as precipitation.

The geographic distribution of the open-basin lakes we interpret as groundwater-influenced appears to relate well to the treatment of Andrews-Hanna et al. (2008), at least at regional scales. Most of the candidate lakes that are V/A_w anomalies are found in Arabia Terra, close to the dichotomy boundary, and in Eridania in the highlands (Figs. 7a, 7d), all regions where groundwater is predicted to reach the surface in the Andrews-Hanna et al. (2008) model (Fig. 7c). Areas where we find lakes with lower V/A_w are also typically in regions where groundwater is less likely to emerge onto the surface in the Andrews-Hanna et al. (2008) model (Figs. 7b, 7d). The predicted locations where water reaches the surface in these global hydrological models broadly coincides with the locations of open-basin lakes that were potentially groundwater-fed. This supports the view that regional-to-global scale groundwater flow may have been important for their formation.

Together with the volume/watershed area ratio, we also compute the ratio of watershed area to lake area, A_w/A, or drainage ratio (Table 2; Fig. 6B) (see Irwin et al., 2007). For lakes where the precipitation–evaporation balance is the key term in their water balance (neglecting the groundwater terms in Eq. (1)), the drainage ratio should be smaller for regions that were comparatively wet (Irwin et al., 2007). This results from the fact that in regions of comparatively wet climate, precipitation is increased relative to evaporation, and basin-filling can occur from comparatively smaller watersheds. (Note that the converse does not hold; basins can have large drainage ratio in either an arid climate or wet climate as long as a minimum threshold in precipitation in excess of evaporation has been reached.) However, as is the case for V/A_w ratio, this

Table 2
Derived parameters for lakes for which we made watershed measurements (lakes without other lakes as important sources, and which have definable watershed boundaries)

Lake #	Area (km^2)	Volume (km^3)	Estimated watershed area (km^2)	Watershed area/lake area	Volume/ watershed area (m)
5	1.60E+02	1.50E+01	20,900	130.93	0.72
9	3.60E+03	4.81E+02	25,000	6.94	19.22
10	9.58E+04	3.10E+04	550,000	5.74	56.43
12	1.65E+02	5.74E+00	2400	14.53	2.39
22	3.15E+03	2.72E+02	24,000	7.62	11.32
24	1.50E+03	8.36E+01	21,500	14.35	3.89
28	4.56E+03	1.23E+03	13,000	2.85	94.75
41	8.27E+04	3.02E+04	155,000	1.87	194.99
45	1.22E+03	2.37E+02	18,100	14.84	13.10
46	4.03E+01	1.59E+00	2400	59.53	0.66
47	3.02E+01	6.06E−01	640	21.17	0.95
51	4.93E+05	2.13E+05	2,080,000	4.22	102.38
59	1.43E+03	1.01E+02	7000	4.90	14.43
63	8.62E+01	2.01E+00	3860	44.78	0.52
64	1.28E+02	3.72E+00	5400	42.12	0.69
73	9.11E+02	9.00E+01	16,000	17.57	5.63
74	1.51E+02	1.26E+01	13,000	85.94	0.97
75	4.52E+03	1.16E+03	430,000	95.16	2.70
77	9.27E+02	8.50E+01	20,080	21.65	4.23
78	3.02E+01	1.65E+00	4300	142.39	0.38
80	2.74E+02	9.70E+00	7650	27.91	1.27
82	1.71E+03	4.35E+01	16,000	9.38	2.72
84	5.40E+02	5.69E+01	20,400	37.75	2.79
85	1.08E+03	5.35E+01	28,500	26.50	1.88
86	2.00E+02	3.73E+00	33,250	166.62	0.11
88	8.11E+01	1.01E+00	600	7.40	1.68
90	4.25E+02	1.34E+01	6100	14.36	2.20
96	9.36E+01	3.99E+00	4400	47.02	0.91
99	2.72E+02	1.48E+01	20,900	76.86	0.71
100	7.71E+01	1.29E+00	7400	96.03	0.17
112	1.99E+02	4.88E+01	27,000	135.57	1.81
116	7.38E+01	3.93E+00	570	7.73	6.89
119	1.83E+03	9.43E+02	3500	1.92	269.41
124	1.35E+02	2.53E+00	950	7.02	2.66
127	1.02E+03	4.15E+01	7750	7.60	5.35
130	1.88E+02	4.50E+01	16,400	87.30	2.75
137	4.18E+01	1.56E+00	8000	191.31	0.19
148	6.00E+02	8.71E+00	3831	6.39	2.27
149	2.56E+02	1.29E+01	2600	10.14	4.96
151	2.60E+03	2.50E+02	24,000	9.25	10.44
154	2.02E+02	8.22E+00	6700	33.13	1.23
155	3.64E+02	2.08E+01	27,000	74.13	0.77
157	2.16E+02	6.36E+00	3000	13.87	2.12
162	1.75E+02	3.72E+00	8000	45.67	0.46
164	2.61E+02	1.59E+01	5500	21.04	2.89
166	3.42E+02	1.11E+01	7800	22.80	1.43
167	1.44E+02	6.82E+00	2000	13.92	3.41
169	1.37E+02	4.18E+00	2400	17.49	1.74
170	3.85E+02	6.14E+01	5500	14.30	11.16
171	3.38E+04	4.84E+03	210,000	6.21	23.06
172	1.20E+02	1.78E+00	615	5.12	2.89
173	3.75E+01	8.03E−01	142	3.78	5.65
174	7.83E+01	1.12E+00	525	6.71	2.14
175	1.43E+02	7.04E+00	2200	15.41	3.20
176	5.91E+01	1.16E+00	3750	63.40	0.31
179	4.93E+02	1.95E+01	3800	7.70	5.14
180	1.89E+02	6.38E+00	620	3.29	10.28
181	3.56E+02	1.31E+01	3400	9.55	3.85
182	1.88E+01	1.44E−01	970	51.72	0.15
184	3.86E+02	2.74E+01	5430	14.08	5.05
185	1.07E+02	4.89E+00	1380	12.93	3.54
186	6.58E+01	1.82E+00	810	12.31	2.24
187	6.17E+02	5.95E+01	4900	7.94	12.15
188	6.19E+04	3.23E+04	106,000	1.71	305.10
189	2.13E+02	5.40E+00	1900	8.94	2.84
190	8.29E+02	4.40E+01	2800	3.38	15.72
191	1.23E+02	2.29E+00	1700	13.77	1.35
192	1.43E+03	5.10E+02	4650	3.25	109.59
194	1.17E+01	1.73E−01	234	20.08	0.74
197	5.45E+02	5.82E+01	1260	2.31	46.17
198	6.36E+01	1.96E+00	2700	42.47	0.73
202	4.12E+03	2.59E+02	8000	1.94	32.32
203	4.29E+00	2.24E−02	36	8.39	0.62

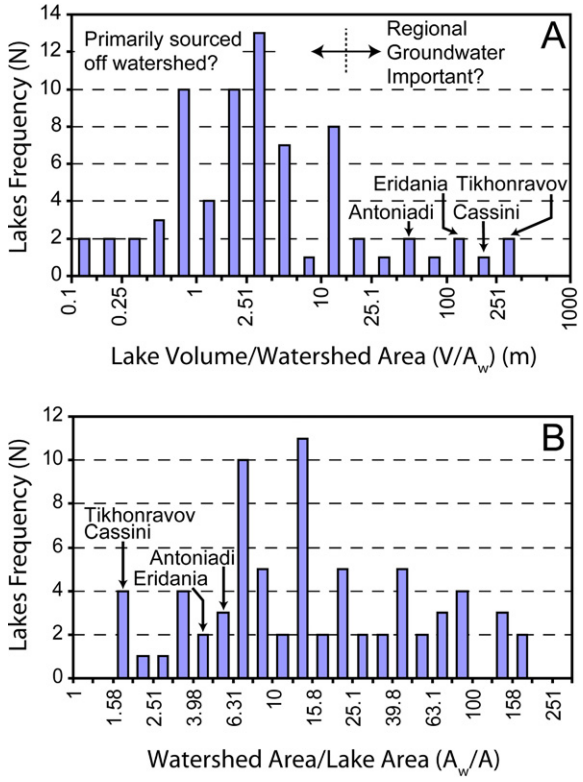

Fig. 6. (A) The frequency distribution of the volume/watershed area ratio for lakes where we measured watersheds. Note the logarithmic scale. Some lakes, especially the large lakes that are labeled (Fig. 4), have volume/watershed ratios that are two orders of magnitude greater than the median value. (B) The frequency distribution of the watershed area/lake area ratio (drainage ratio) for lakes where we measured watersheds. Note the logarithmic scale. In this metric, many of the hypothesized groundwater-fed lakes have very small watersheds relative to their lake area.

quantity can also be altered if groundwater inputs were important; many of the lakes that have high values of V/A_w also have low values of A_w/A (Fig. 6B), as is expected given the correlation between volume and area (Fig. 2d). We thus focus our analysis on lakes with $V/A_w < 15$, where precipitation is likely to have been the most important source.

Lakes on Mars where we have watershed measurements and that have lake volume-watershed area ratios <15 are shown in Fig. 8. Here we highlight a few broad trends that can be observed:

(1) The 22 lakes between 40° W and 80° E longitude have watershed area to lake area (A_w/A) ratios of ~15 compared to ~48 for the 38 other lakes elsewhere on Mars where $V/A_w < 15$. This distribution suggests that this broad region was comparatively "wet" (more precipitation and/or surface runoff), consistent with the location of the longest lake chains (Fig. 3) formed on Mars (see also Irwin et al., 2007).

(2) Between longitude 70° E and 150° E in the eastern hemisphere, there is a trend towards smaller A_w/A ratios from south to north (approaching the dichotomy boundary). In this longitude range, the nine lakes between 30° S and 15° S have $A_w/A = 39$, and the 18 lakes between 15° S and 0° S have $A_w/A = 14$. A plausible interpretation for this trend is climate variation from south to north, with the northern part of the region close to the dichotomy boundary and equator somewhat "wetter" than regions further to the south. Potential causes of this variation are orographic effects of the dramatic break in slope at the dichotomy boundary, or enhanced precipitation and runoff production in this region of the equatorial zone, perhaps driven by global circulation patterns such as intertropical convergence.

These data on the variations in character of lakes on Mars as a function of elevation, latitude and longitude, all suggest that the lacustrine sediments forming on the floors of these lakes may be significant records of regional climatic variations on Mars, as they are for terrestrial climate.

3.4. Evidence for resurfacing of lake floors

Valley network systems that are the sources of water in the open-basin lakes generally formed in the late Noachian, near the Noachian–Hesperian boundary (Fig. 9). This period is just before the emplacement of the Hesperian ridged plains, a very widespread unit that covers the floors of the major basins, the Tharsis region, the northern lowlands (Head et al., 2002), and a significant number of low-lying areas, commonly crater floors, in the uplands of Mars (Scott and Tanaka, 1986; Greeley and Guest, 1987). The nature of the Hesperian ridged plains has been interpreted to mean that they are of volcanic origin, predominantly flood basalts (Scott and Tanaka, 1986; Greeley and Guest, 1987). Indeed, extensive exposed feeder dikes have recently been found (e.g., Head et al., 2006a). Soon after their emplacement, these plains were deformed by wrinkle ridges, which are shallow compressional faults formed in competent materials (e.g., Watters, 1988). Because of the proximity in time of the Late Noachian valley network formation and Early Hesperian ridged plains emplacement, we might expect many Noachian basin floors to have been resurfaced during the Early Hesperian.

At least 42 of our cataloged lakes (20%) have wrinkle ridges on their floors, usually in plains-forming material (e.g., Figs. 10, 11; see also #6, #56, #75, #154). Although caution is required when linking the observation of a class of structural features with a particular lithology, most well-characterized, wrinkle-ridged surfaces on the terrestrial planets are in volcanic material; the strength of volcanic plains materials may be uniquely (or at least particularly) conducive to wrinkle ridge formation (Watters, 1991). Thus, the observation of wrinkle ridges on basin floors is strongly suggestive that they have been resurfaced by post-lacustrine volcanic materials that may obscure any primary sedimentary or lacustrine character.

Furthermore, many lakes (61 more, ~30%) have smooth plains units on their floors without obvious wrinkle ridges at image resolutions we utilize. These smooth plains appear to embay basin margins and are interpreted as the youngest material on the basin floor. Other commonly observed characteristics of the smooth plains are lobate margins, a diagnostic appearance in MOLA shot-to-shot roughness data (Kreslavsky and Head, 2000), and small-crater preservation suggesting highly competent material (e.g., Figs. 5, 6). We consider it unlikely that these competent floor materials are sedimentary, as the combination of morphological characteristics described above is usually interpreted to indicate the presence of volcanic material. Thus, there is positive evidence suggesting that approximately half of the hydrologically open-lake basins that we have documented were resurfaced in the Hesperian or later, following lake formation in the Late Noachian. In some cases, the sources of this resurfacing are obvious. For example, Antoniadi crater (Figs. 4d–4f) has clearly been at least partly covered by Hesperian-aged lava from Syrtis Major (Hiesinger and Head, 2004). Other processes may also be effective in burying Noachian materials, including ejecta from later impact craters (Cohen, 2006) and regional or global-scale mantling units (Soderblom et al., 1973; Mustard et al., 2001).

The inference that resurfacing has occurred in many lake-related basins is not new. Goldspiel and Squyres (1991) recognized

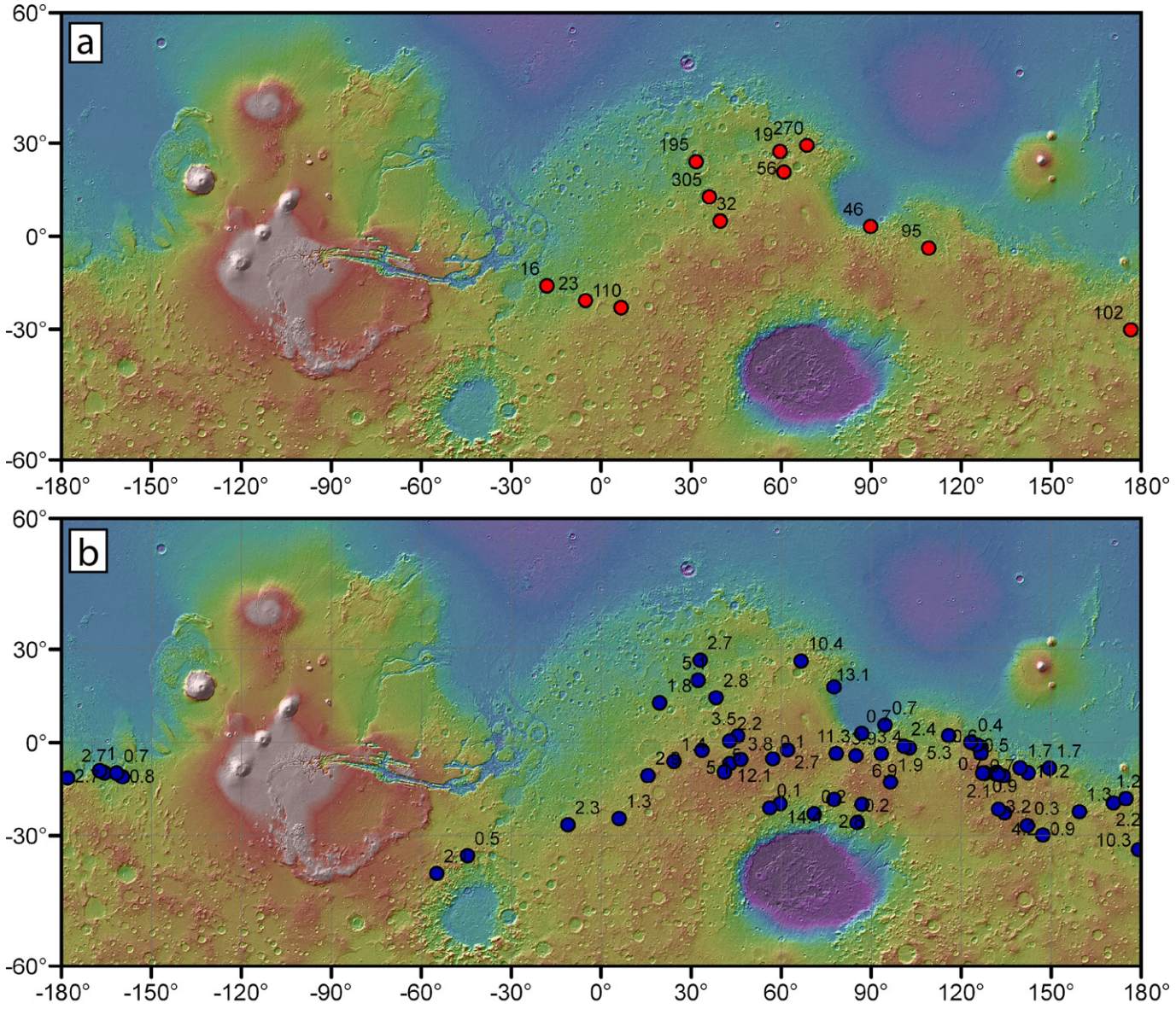

Fig. 7. (a) Lakes in Table 2 with $V/A_w > 15$ that we interpret as likely to have been significantly fed by groundwater (labels are V/A_w for the lakes). Note that the large lakes with the highest V/A_w are found in north-central Arabia Terra and Eridania (see Fig. 4). (b) Lakes in Table 2 with $V/A_w < 15$, likely to be predominantly fed by precipitation; labeled values are V/A_w. (c) Groundwater evaporation rates from Andrews-Hanna et al. (2008) (maximum value (red): 0.15 mm/yr). Locations where groundwater is evaporating in the Andrews-Hanna et al. model are proxies for groundwater reaching the surface. (d) Combination of parts (a), (b), and (c). Note the broad regional agreement between where potential groundwater-fed lakes (from a, shown in red) and where the Andrews-Hanna et al. models suggest that groundwater was reaching the surface (from c, key regions outlined). The converse relationship is also strong; where lakes have low V/A_w ratios (in blue, from b), models suggest a deep groundwater table that does not intersecting the surface. (For interpretation of the references to color in this figure legend, the reader is referred to the web version of this article.)

that "in many instances, the sedimentation [on] basin floors appear to be covered by volcanic extrusions … post-dat[ing] the period of fluvial activity." In particular, noting the signs of volcanism (wrinkle ridges) on the Gusev crater floor, they interpreted the floor of Gusev to have been volcanically resurfaced. Recently, this interpretation was born out by the *in situ* observations of the Mars Exploration Rover Spirit (Squyres et al., 2004).

Additional strong evidence for post-lacustrine resurfacing on former lake floors comes from crater statistics. Recent work has helped to demonstrate quantitatively that the valley networks that fed the lakes in this study date to the time of the Late Noachian, near the Noachian–Hesperian boundary (Fassett and Head, 2008) (Fig. 9). In the current study, we have obtained reliable crater statistics on a few paleolake floors that suggest resurfacing when combined with other characteristics (e.g., Fig. 10). These crater counts yield crater-retention ages of crater and basin floors that in various cases date from the Early Hesperian to Early/Mid Amazonian boundary. These data are somewhat less reliable statistically than the valley network data (Fassett and Head, 2008) because the lake floors are small areas, necessitating reliance on smaller craters. Nonetheless, these new counts are consistent with crater counts and ages determined by previous workers (Cabrol and Grin, 2001; Irwin and Howard, 2002) and with our interpretation that about one-half of the basins in this study have been resurfaced following the period of fluvial activity represented by the valley network systems.

The well-studied breached crater in Memnonia (Fig. 11) characterized by an interior terrace and outlet valley (Forsythe and Zimbleman, 1995; Cabrol and Grin, 1999, 2001; Leverington and Maxwell, 2004; Irwin et al., 2005a) is of particular interest

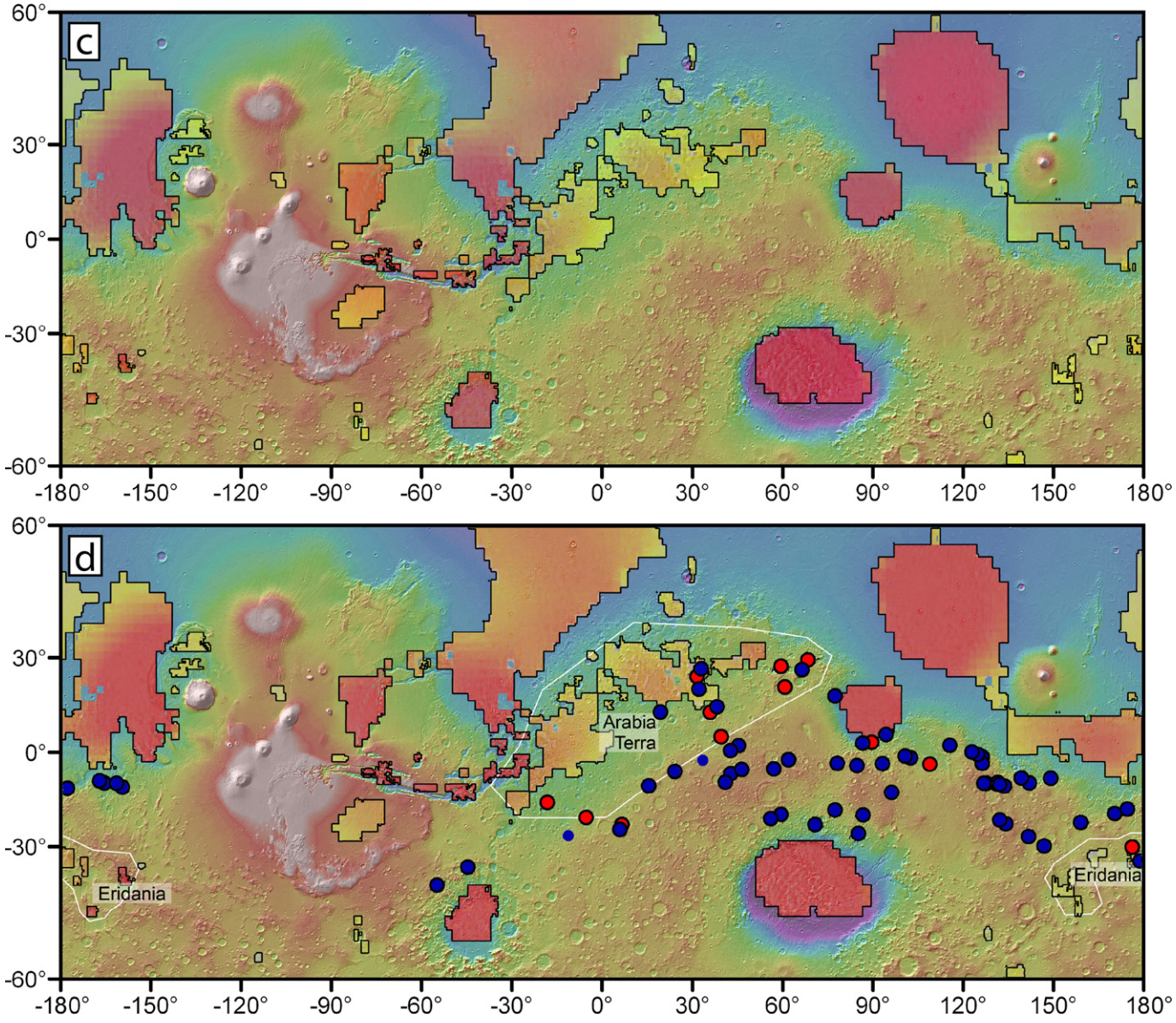

Fig. 7. (*continued*)

in understanding the potential resurfacing of lake basin floors. Leverington and Maxwell (2004) advocated a volcanic origin for the inlet, terrace, and outlet valley, with flow of lava replacing the flow of water to form a paleolake. On the basis of topography and geologic setting, Irwin et al. (2005a) convincingly refuted the interpretation that the valleys and terraces associated with this crater could have formed by volcanic processes. Irwin et al. (2005a) note that the formation of the outlet valley from this crater required either (a) flooding the crater to substantial depth, which if the relevant fluid was lava, would likely have left evidence at high elevations, or (b) as a lava tube, which is inconsistent with the observed morphology of the outlet valley.

However, Irwin et al. (2005a) do state that "minor volcanic resurfacing of the terraced crater floor or other localized basin surfaces cannot be ruled out with existing data." Indeed, we think that such volcanic resurfacing is likely on many crater floors, because many of the observations of Leverington and Maxwell (2004) are consistent with resurfacing by a thin volcanic unit, rather than with a "system and valley-wide lava flow." These observations include: (1) the surface textures of the floor unit, also seen in other nearby basins and similar to ridged plains elsewhere on Mars, (2) the presence of wrinkle ridges that are typically indicative of volcanic material (e.g., Gusev), and (3) the strong preservation of the small-crater population (see Fig. 11). Two additional observations suggest that resurfacing occurred here. First, the floor has a crater population well-described by isochrons and consistent with an Early Amazonian age (Fig. 11c). This differs significantly from the crater population and age of highland valley networks (Fig. 9; Fassett and Head, 2008). Second, we believe that flow margins are recognizable inside the basin (especially along the northwest and southeast terrace walls), where the floor unit embays the terrace (Fig. 11b; compare with Fig. 10d). From these contacts, we estimate that the floor unit that we interpret to be volcanic fill as ~30 m thick.

This potential resurfacing and modification of lake floors alters the lacustrine record in a variety of ways. One effect is that the morphometric properties that we measure are somewhat altered (Tables 1 and 2). In particular, the volumes that we measure may have been reduced by post-lacustrine infilling, especially for basins like Antoniadi crater (Fig. 4d), where the thickness of volcanic fill on the basin floor appears non-negligible. Lake areas also may be

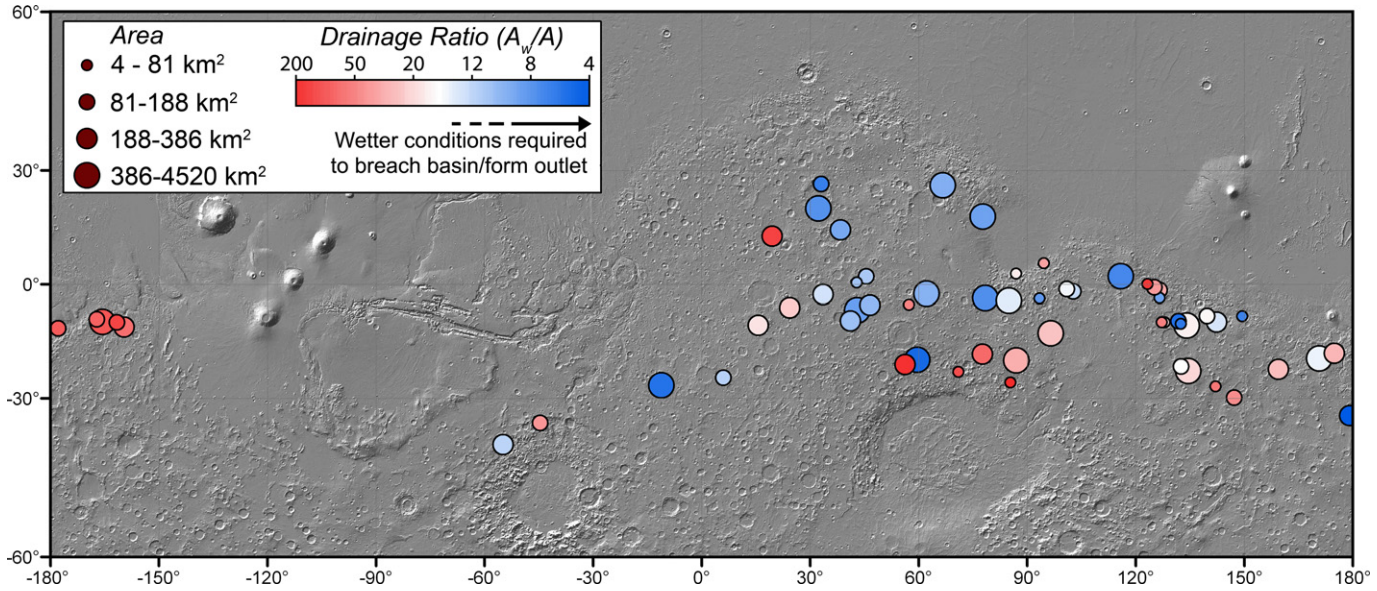

Fig. 8. Map of the drainage ratios for the candidate lakes with watershed measurements where $V/A_W < 15$. Color here is a function of A_w/A, where lakes with smaller watersheds relative to their size are bluer. Locations with low A_w/A ratios may have had more precipitation relative to evaporation during the Noachian (see text). Dot size is a function of lake area (quantiles).

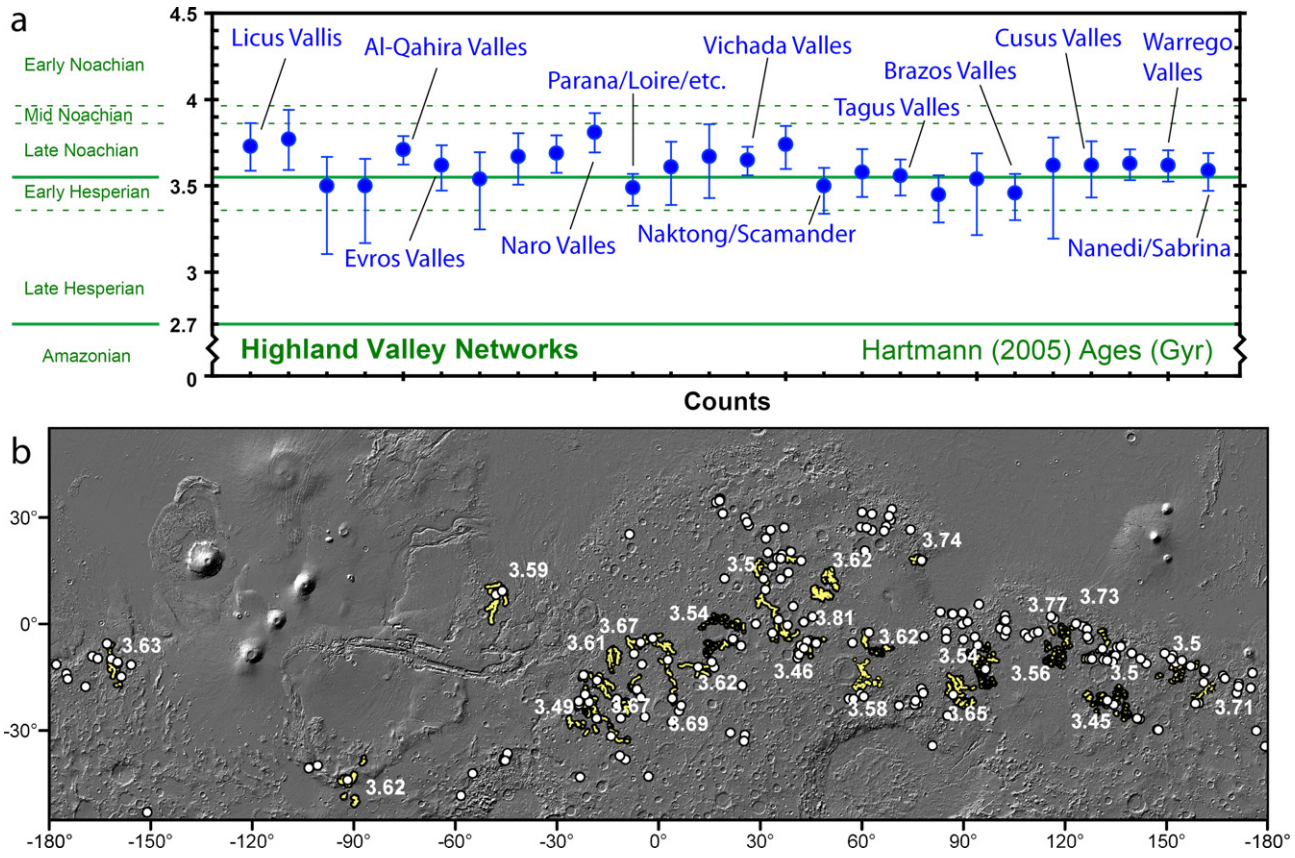

Fig. 9. (a) Distribution of ages for the highland valley networks derived from size-frequency distributions determined using buffered crater counting (Fassett and Head, 2008). Absolute ages are model-dependent and referenced to the isochrons of Hartmann (2005). The end of valley network formation appears to be constrained to a period ending at approximately the Noachian–Hesperian boundary. (b) Distribution of analyzed valleys (lines) and lakes (dots), with model ages superposed in Gyr.

somewhat affected. Nonetheless, these changes are unlikely to affect the general conclusions of this study.

A second important effect of the basin floor resurfacing is that clearly preserved and exposed fluvio-lacustrine sediments are relatively rare. In the data that we examine, ~50% of the lakes show evidence for resurfacing, and only 16 of the 210 catalogued lakes (~8%) show clear evidence for outcropping sediment. Most of these have been previously recognized, and the most obvious examples have already been discussed in some detail (see Irwin et al., 2005a, and references therein). Based on the degree to which high-resolution data have revealed resurfacing of candidate ancient lakes, and the rarity of sediments observed in open lake basins,

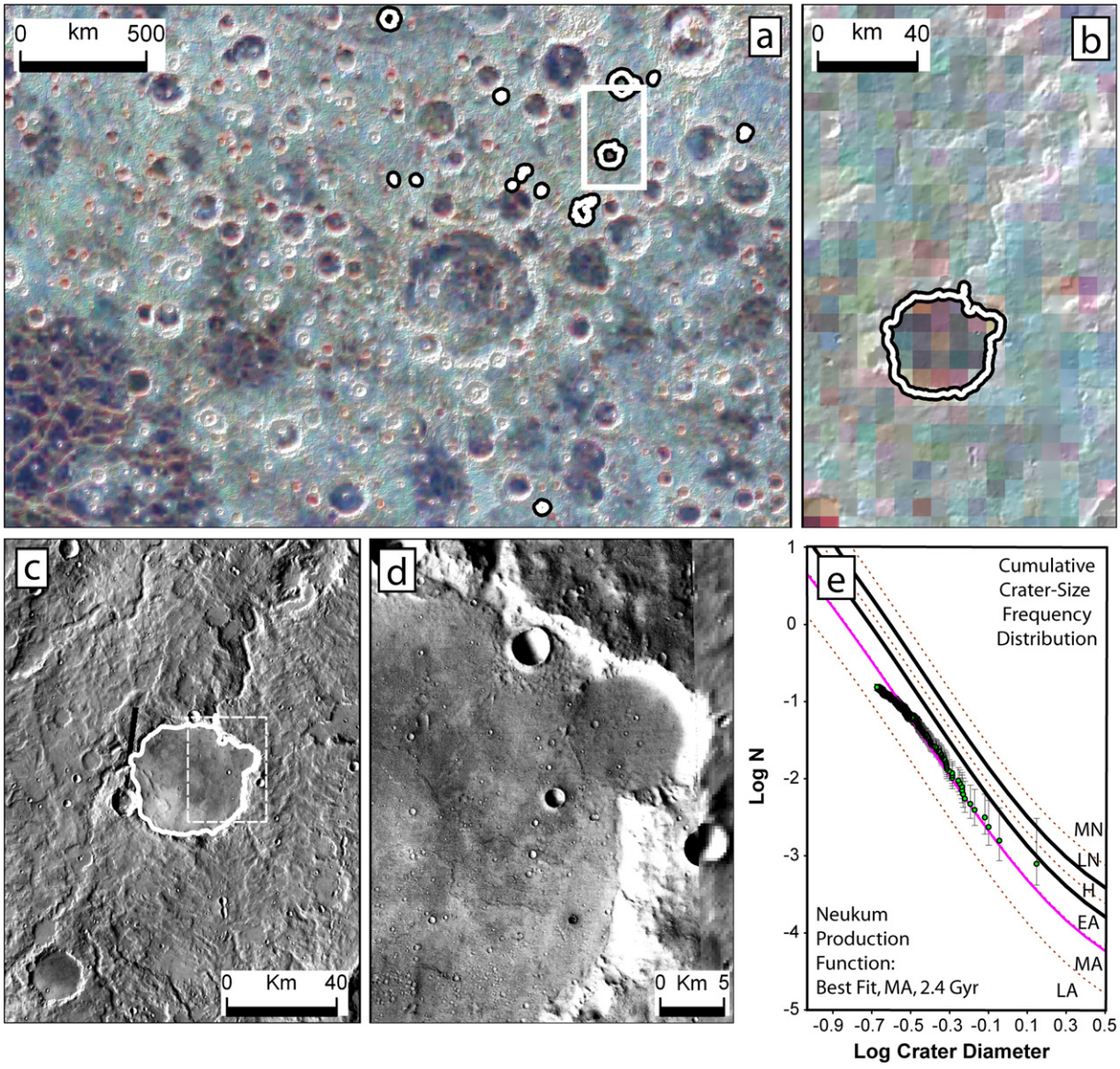

Fig. 10. (a) Roughness map at three length scales from Kreslavsky and Head (2000). Smooth volcanic units such as the wrinkle-ridged plains of Hesperia Planum tend to be dark. (b) Roughness map of basin #72, showing the characteristic dark signature of a volcanic unit. (c) THEMIS IR image of basin #72, showing the outlet valley that defines it as an open basin. (d) HRSC nadir image h1960_0000 of basin #72, showing the smooth floor unit that appears to embay the outlet valley and crater wall, retaining its small crater population in a manner consistent with volcanic deposits. (e) Cumulative crater size-frequency distribution of the floor unit of basin #72, revealing an age at the Early Amazonian/Mid-Amazonian boundary (~2.4 Gyr) based on small craters. A similar result (but younger absolute age, ~1.8 Gyr) is obtained using the Hartmann (2005) age model.

care must be exercised in the choices for exploration of valley network deposits and former lake floors. Ideally, exploration of lacustrine environments should focus on locations that have the potential for exposed sedimentary material and structure, as well as mineralogy that may provide evidence for the nature of the environment, like chloride minerals (Osterloo et al., 2008) or clays (e.g., Ehlmann et al., 2008). Orbital instruments have shown that clear examples exist even among the modest population of locations with exposed sedimentary material (e.g., Malin and Edgett, 2003; Moore et al., 2003; Fassett and Head, 2005; Irwin et al., 2005a; Ehlmann et al., 2008; Grant et al., 2008).

4. Discussion

4.1. The role of groundwater

The distribution and characteristics of valley networks, lakes, lake chains, and their catchments can provide important information about the Noachian hydrologic cycle. The average surface temperature today on Mars is only ~215 K at the equator, which means that the temperature of the crust is well below the freezing point of water to substantial depth. For this reason, a thick cryosphere (>2 km) is expected to exist on modern Mars, where water occurring at these depths would freeze (Clifford, 1993). Under current climatic conditions, the hydrological system and cycle can be thought of as horizontally layered, with a global cryosphere separating any groundwater at depth from significant communication with water at the surface (Fig. 12A). The current surface hydrological cycle consists of reservoirs in the atmosphere, the polar caps, and the regolith. Water cycles through these three reservoirs as a function of changing seasonal insolation and longer-term tends driven by variations in spin-axis and orbital parameters. These conditions were probably characteristic of Mars throughout much or all of the Amazonian and Hesperian based upon the geological record (e.g., Head et al., 2004, 2005, 2006b; Hauber et al., 2008; Head and Marchant, 2008).

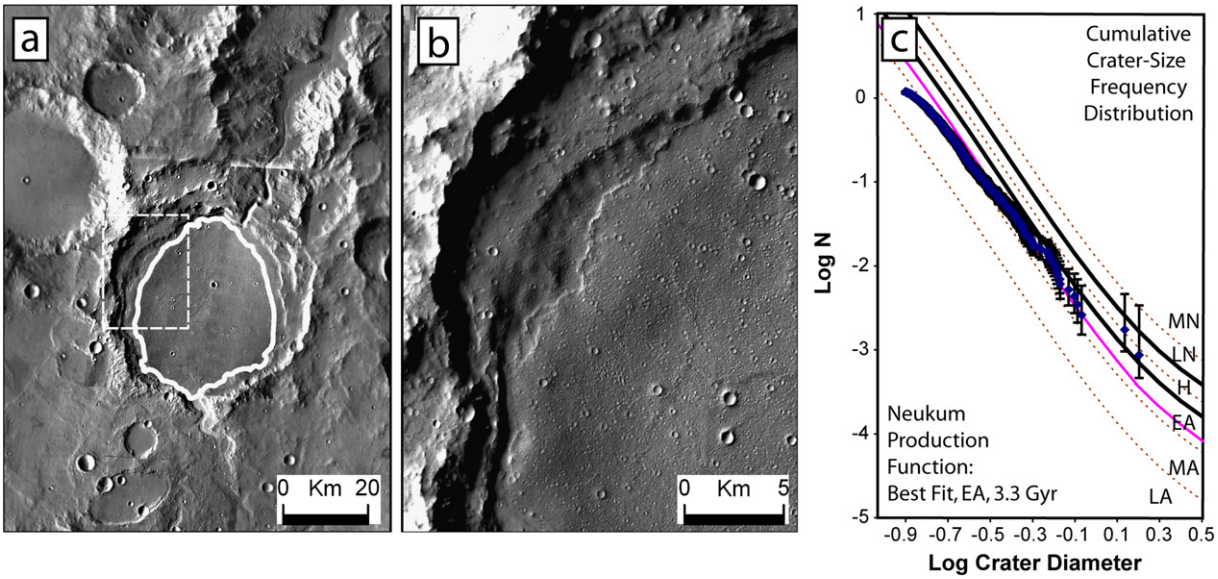

Fig. 11. (a) THEMIS IR and THEMIS VIS images of a well-studied crater lake in Memnonia (our basin #4). (b) In detail, the unit on the floor of this crater appears to embay the terrace along its walls. (c) Cumulative crater size-frequency distribution of the floor unit of the Memnonia crater (#4), revealing an Early Amazonian age (~3.3 Gyr) based on small craters. The same geological period is obtained using the Hartmann (2005) age model (Hartmann age of ~2.7 Gyr).

Prior to this time, a higher geothermal gradient together with a warmer, wetter surface environment during at least some of the Noachian may have led to a vertically integrated hydrological system, with no global cryosphere, and vertical communication between the surface and the subsurface through an extensive and varying vadose zone (Figs. 12B, 12C) (Head et al., 2003). To have this vertically integrated system, the cryosphere must have been absent from at least some of Mars, especially in mid-to-low latitudes, allowing water to infiltrate the surface and move through the crust. This recharge would require surface temperatures over much of Mars warmer than today (close to, or greater than, the freezing point of water), to pin crustal temperatures above 273 K (Forsythe and Zimbleman, 1995; Carr and Malin, 2000). It also requires that the groundwater system was interconnected at regional-to-global scales (Clifford, 1993; Clifford and Parker, 2001). Recharge in the Late Noachian may have been driven by the valley networks at comparatively high elevations, where they were influent and losing water into a vadose zone (Figs. 7 and 12C). Valleys at lower elevations where the groundwater table was shallower may have been effluent, with groundwater contributing to their flux (Fig. 12). Lakes and lake chains may have been influenced in the same manner. For groundwater to be a net source to these lakes, as suggested by our data, regional-to-global-scale groundwater transport was necessary, and the surface and subsurface hydrosphere must have been linked during at least part of the Late Noachian.

The large volumes of some lakes relative to their watershed areas suggest that groundwater was a net contributor to their filling. Groundwater input may have been especially important for the largest lakes on Mars. Basin floor morphology helps to support the view that groundwater played a role in the development of these largest lakes. A common feature of some of these lakes (#11, #16, #18, #19, #28, #51) is the presence of knobby material on their floors. The most reasonable explanation for the formation of this knobby material is removal of hydraulic support following groundwater removal (e.g., Head and Pratt, 2001; Irwin et al., 2002, 2004a), akin to the processes of chaos formation hypothesized to lead to outflow channel formation (Carr, 1979). In addition, some candidate groundwater-fed lakes (#9) have limited signs of surface sources of water, lacking evidence for abundant source valleys for water input.

If regional groundwater was a more significant contributor to some lakes than others, the water chemistry of these lakes may have been more influenced by the crust than lakes mostly influenced by local surface input. Specifically, groundwater that underwent regional transport and had long residence times in the basaltic crust of Mars may have had time to become more solute rich than waters limited by chemical weathering rates at the surface. Terrestrial observations and modeling show greater dissolved solids and mineralization in lakes with regional deep groundwater as important sources, compared to those lakes controlled by runoff or more local groundwater (e.g., Winter and Carr, 1980). Although much remains unknown weathering environment of early Mars, it is possible that the water chemistry of potential groundwater-fed lakes (Fig. 12C) and those fed predominantly by precipitation may have been different, and that these differences may be preserved in the geochemistry and mineralogy in their lake sediments. It is possible that these differences may be detectable by orbital instruments, such as the Compact Reconnaissance Imaging Spectrometer for Mars (CRISM).

Furthermore, several of the largest anomalous basins occur in relatively low terrains near the dichotomy boundary. Some of these lakes feed valleys in regions of fretted terrain (e.g., Carr, 1996). Fretted valleys have a complex geological history, including modification by structural processes such as flexure-induced extension, fracturing (Watters, 2003; Watters and McGovern, 2006), collapse and disaggregation (Irwin et al., 2004b), as well as recent glacial processes (e.g., Head et al., 2006b). However, liquid water also appears to have been responsible for the formation of some fretted valleys (McGill, 2000). Indeed, outlets from many of the open-basin lakes in this study (#9, #11, #21, #28, #115, #118, #119, #120, #152) appear to directly feed fretted valleys (e.g., Figs. 4d–4f). Many of these open basins connected to fretted terrain were potentially groundwater-fed, and a role for groundwater in these source lakes is consistent with sapping playing a role in the formation of some fretted valleys (see, e.g., Harrison and Grimm, 2005). Although fretted valleys have been formed and modified by a multitude of processes, it is thus clear from our catalog that overtopping of open-basin lakes, as well as other fluvial processes, influenced at least some of the fretted valleys we presently observe.

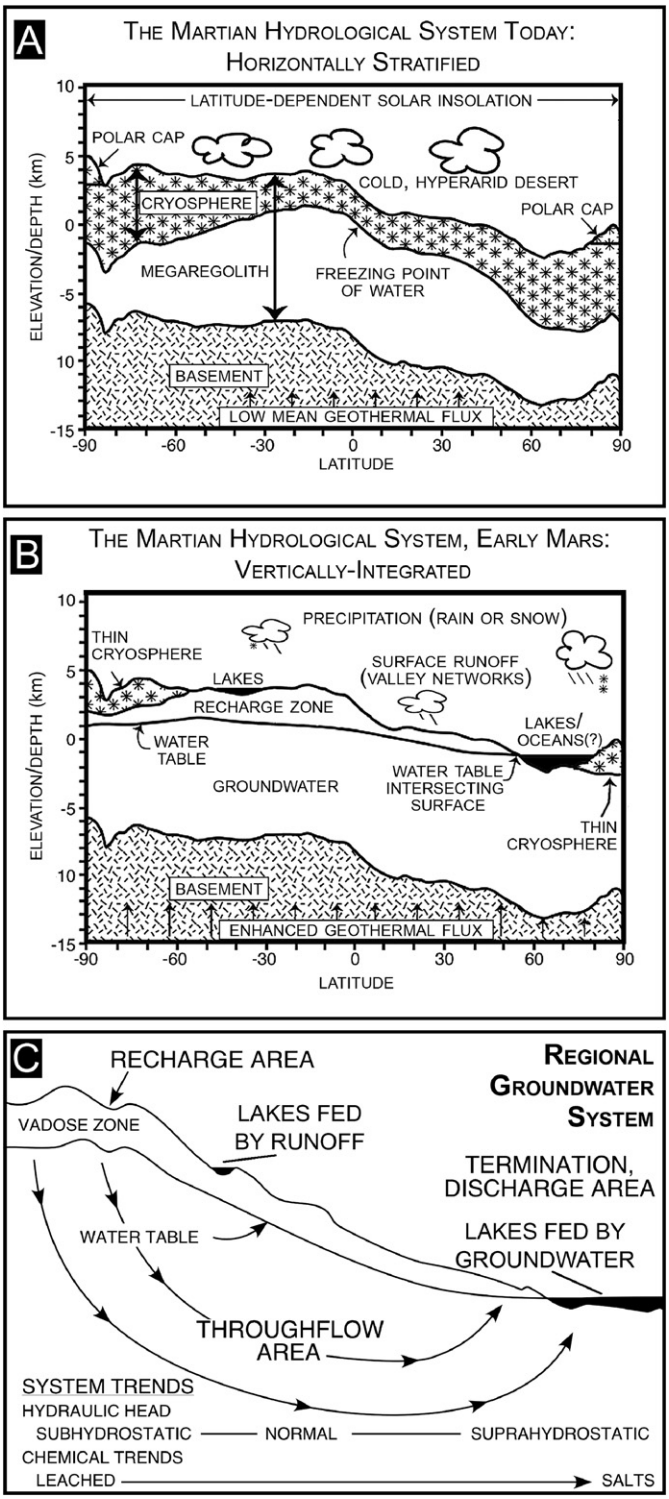

Fig. 12. (A) A schematic diagram illustrating the latitude-dependent hydrosphere of Mars today. Over the entire planet, water ice on the surface is segregated from any subsurface water reservoir by a thick region of the crust where the temperature is permanently below the freezing point of water (the cryosphere). (B) A schematic diagram illustrating the nature of the early martian hydrosphere. The interpretation that some lakes were groundwater-fed would require that recharge of groundwater was possible and that the subsurface and surface hydrospheres were vertically integrated. (C) Diagram illustrating a single-flow, regional-scale groundwater system. Lakes and valleys in the uplands are predominantly fed by precipitation transported as runoff and local groundwater from their watersheds. At lower elevation, the regional groundwater system intersects the surface, feeding a lowland lake. The upland lakes and lowland lakes are expected to have differences in chemical trends reflecting their different water sources.

4.2. Surface water volumes and the water inventory of Mars

Analyzing the water inventory of Mars through time is important for understanding the evolution of the planet and for formulating limits on the initial inventory of water (e.g., Carr, 1996). The measured volumes of lakes in our catalog provide lower limits on surface water inventories (see Table 1). The precise amount of water depends on whether or not the lakes were all active at once. As an upper limit, we sum the volumes of lakes in our catalog and derive a total volume of 4.2×10^5 km^3, which is equal to a ~3 meter-thick layer spread over the globe, or global equivalent depth (GED). This is well within the current water inventory of Mars, and it is about an order of magnitude less water than is currently sequestered in both of the polar caps (~25–30 m GED) (Smith et al., 1999).

A more substantial component of the water inventory follows from the interpretation that regional-to-global-scale groundwater flow fed some of the lakes during the Noachian. If correct, this scenario implies that the subsurface water inventory was significant and that groundwater was not sequestered at great depths beneath a planet-wide cryosphere. Instead, groundwater reservoirs were sufficiently large to form a water table at depths shallow enough to intersect the surface at the some locations, such as the candidate groundwater-fed lakes (Figs. 12, 13). Estimating a detailed minimum groundwater inventory from this observation alone is model dependent; however, an order of magnitude estimate based on using parameters of the hydrological model developed by Hanna and Phillips (2005) is ~200–600 m GED.

On the basis of these same considerations, however, we speculate that groundwater may also have reached the surface and ponded in the lowlands north of the dichotomy boundary and in the deeper basins on Mars (Hellas, Argyre, Isidis) (Fig. 12B) (Clifford, 1993; Clifford and Parker, 2001). Indeed, Argyre may have been an open basin at one time (e.g., Parker and Gorsline, 1991), although its putative outlet through Uzboi Valles is now heavily degraded by later impacts (Hiesinger and Head, 2002). The view that these regions of low topography were likely locations for groundwater to reach the surface is consistent with what is observed in the recent modeling of Andrews-Hanna et al. (2008) (Fig. 7). However, the formation of deep bodies of water in these locations depends on the local water balance (the surface and groundwater inputs versus evaporation and groundwater losses), and on a permeable groundwater connection between the highlands and lowlands (Grimm and Harrison, 2003). Filling these topographically low surface reservoirs would add hundreds of meters GED to the required global water inventory (Carr and Head, 2003).

4.3. A conceptual framework for Noachian open-basin lake formation

On the basis of our analysis, we outline a broad conceptual framework for the hydrological conditions of the Late Noachian (Fig. 7). First, precipitation (rain or snow) collected in the highlands and flowed overland through valley networks to collect in lakes. The distribution of lakes (Fig. 1) suggests that precipitation was widespread across the planet, although differences in the lake area/watershed area ratio (Fig. 4c) imply that there were variations in the balance of precipitation and water-loss mechanisms (evaporation, infiltration) in different regions. For example, Arabia and areas near the dichotomy may have been "wetter" (Section 3.3) than other regions of the planet.

Runoff, either directly from rain or from melting of snow or ice, eroded the valley networks. Water in these valleys collected on the surface in local catchments, forming lakes. Our data suggest that precipitation was the dominant source of water for most lakes at high elevations in the southern highlands, since these lakes

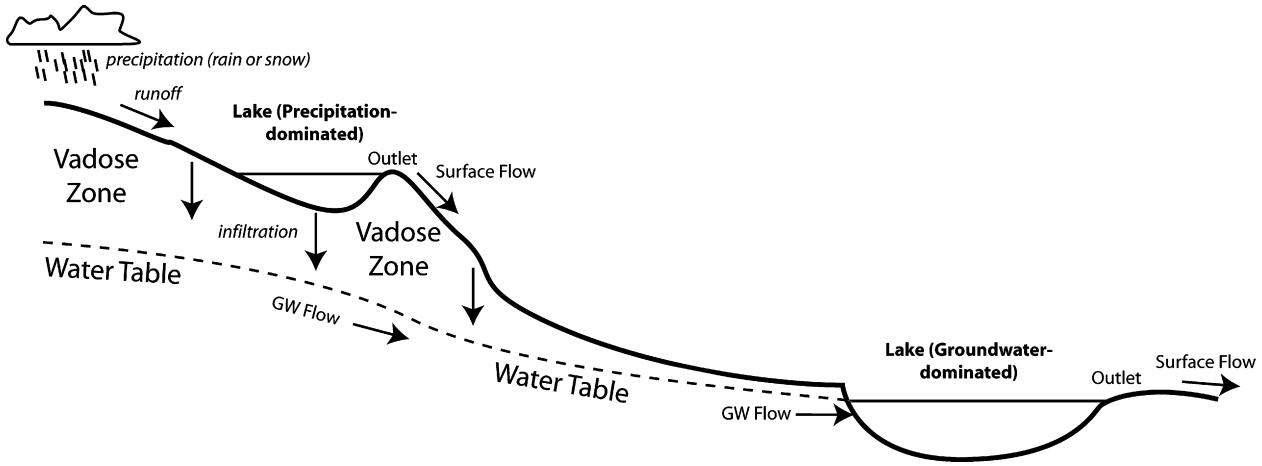

Fig. 13. A conceptual model for the hydrology of early Mars. Our data support the interpretation that the largest lakes, generally at low elevations, were fed by groundwater recharged at higher elevations in the highlands.

have volumes proportional to their watershed area. Groundwater recharge may have been concentrated in these upland regions where lakes were fed by precipitation, as both valleys and lakes may have been influent in these locations, losing water through a vadose zone to a deep water table (Figs. 12B, 12C, 13). Irwin et al. (2005b) measured formative discharge in martian channels and found that the discharge appears to have increased less quickly with watershed area than for in humid-zone rivers on Earth. This work implies that on early Mars, the partitioning of precipitation or melting into runoff was comparatively inefficient (Irwin et al., 2005b), consistent with this view that in many upland regions, valley networks and lakes may have been influent. Nonetheless, in the case of each open-basin lake, surface and subsurface water input must have exceeded infiltration and evaporation in order to allow the basins to fill, overflow, and form the observed outlets.

Lake chains provide a further important constraint. After ponding occurred, outlet valleys commonly drained one lake and connect to a downstream depression forming another lake. In order for lake chains to occur, water must have been continuously present throughout the entire system to carve the connecting valleys and fill successive lakes in the chain (e.g., Fig. 3). As lake chains reached the lower parts of the cratered highlands, the water table began to exert greater influence on the surface hydrology, especially in Arabia Terra, Eridania, and areas of low topography near the dichotomy boundary (Fig. 7). Groundwater was very likely a net source of water to lakes at the lower reaches of long valley–lake systems (such as the Naktong/Scamander/Mamers chain; connected to Cassini and Tikhonravov, Figs. 4a, 4g), as well as to deep craters that were not integrated into broad highland networks but are the source of valleys at the dichotomy boundary (e.g., Antoniadi, Fig. 4d). This type of influent groundwater system in high-elevation terrains and effluent regional groundwater systems at lower elevations is consistent with the observed geometry in many places on Earth.

It is possible that other environmental scenarios may be consistent with what our observations, such as a scenario which invokes climate excursions following large impacts (Segura et al., 2002; Colaprete et al., 2004). For such a model to be viable, it must be consistent with (1) the observed timing of valley network formation and presumed lacustrine activity (Fassett and Head, 2008); (2) the widespread geographic distribution of valley networks and lakes across the planet (Fig. 1); (3) the integrated activity along substantial valley–lake-chain systems (e.g., Fig. 3); (4) the filling of individual basins with substantial volumes (e.g., Fig. 4), which might take a lengthy period of time to fill; and (5) vertical integration of the surface and subsurface hydrology via recharge and discharge, if, as our data suggest, groundwater was important to the hydrology of early Mars. Further study is needed to evaluate whether the impact hypothesis or other scenarios can meet these constraints.

5. Conclusions

We present a new catalog of 210 open-basin lakes on Mars, the majority of which are newly recognized. We conclude that:

1. The majority of the open-basin lakes that we delineate were part of integrated lake-chain systems.
2. Morphological measurements of these lakes and their outlets allow us to determine the minimum amount of water necessary to flood these basins. The largest lakes on early Mars were comparable in size to the largest lake basins (or small seas) of modern Earth.
3. Crater counts and morphological indicators imply that resurfacing of lake floors has been very widespread. This late activity may make access to primary Noachian lake materials difficult in many locations, although excellent examples are known.
4. The observation that watershed area is directly proportional to lake volume suggests that most of the catalogued lakes were fed by precipitation and runoff.
5. In some cases, including the largest lakes, groundwater appears to have been an important net source. Our interpretation of the location of groundwater-sourced lakes is broadly consistent with predictions of current groundwater models.
6. Our conceptual model of the late Noachian hydrological system and cycle consists of influent valleys and lakes in the uplands and larger lakes in the lowlands sourced by effluent from global-to-regional groundwater flow.

Acknowledgments

We are grateful for careful and thorough reviews by Ross Irwin and Stephen Clifford. Thanks to James Russell, James Dickson and Joseph Levy for helpful discussions and to Jeffrey Andrews-Hanna for permission to use Fig. 7. This work was funded with support from the NASA Mars Data Analysis Program (NNG04GJ99G), the NASA Mars Express Participating Scientist Program (JPL1237163), the NASA AISR program (NNGO5GA61G) (JWH) and the NASA Graduate Student Research Program (CIF).

Supplementary material

The online version of this article contains additional supplementary material.

Please visit DOI: 10.1016/j.icarus.2008.06.016.

References

Ambrosetti, W., Barbanti, L., 2002. Physical limnology of Italian lakes. 2. Relationships between morphometric parameters, stability and Birgean work. J. Limnol. 61, 159–167.

Andrews-Hanna, J.C., Phillips, R.J., Zuber, M.T., 2007. Meridiani Planum and the global hydrology of Mars. Nature 446, 163–166.

Andrews-Hanna, J.C., Zuber, M.T., Phillips, R.J., 2008. Early Mars hydrology: Valley networks and evaporites. Lunar Planet. Sci. 39. Abstract 1993.

Baker, V.R., Milton, D.J., 1974. Erosion by catastrophic floods on Mars and Earth. Icarus 23, 27–41.

Banerdt, W.B., Vidal, A., 2001. Surface drainage on Mars. Lunar Planet. Sci. XXXII. Abstract 1488.

Cabrol, N.A., Grin, E.A., 1999. Distribution, classification, and ages of martian impact crater lakes. Icarus 142, 160–172.

Cabrol, N.A., Grin, E.A., 2001. The evolution of lacustrine environments on Mars: Is Mars only hydrologically dormant? Icarus 149, 291–328.

Carr, M.H., 1979. Formation of martian flood features by release of water from confined aquifers. J. Geophys. Res. 84, 2995–3007.

Carr, M.H., 1996. Water on Mars. Oxford University Press, New York. 229 pp.

Carr, M.H., Head, J.W., 2003. Oceans on Mars: An assessment of the observational evidence and possible fate. J. Geophys. Res. 108, doi:10.1029/2002JE001963. 5042.

Carr, M.H., Malin, M.C., 2000. Meter-scale characteristics of martian channels and valleys. Icarus 146, 366–386.

Christensen, P.R., Jakosky, B.M., Kieffer, H.H., Malin, M.C., McSween Jr., H.Y., Nealson, K., Mehall, G.L., Silverman, S.H., Ferry, S., Caplinger, M., Ravine, M., 2004. The Thermal Emission Imaging System (THEMIS) for the Mars 2001 Odyssey Mission. Space Sci. Rev. 110, 85–130.

Clifford, S.M., 1993. A model for the hydrologic and climatic behavior of water on Mars. J. Geophys. Res. 98, 10973–11016.

Clifford, S.M., Parker, T.J., 2001. The evolution of the martian hydrosphere: Implications for the fate of a primordial ocean and the current state of the northern plains. Icarus 154, 40–79.

Cohen, B.A., 2006. Quantifying the amount of impact ejecta at the MER landing sites and potential paleolakes in the southern martian highlands. Geophys. Res. Lett. 33, doi:10.1029/2005GL024963. L05203.

Colaprete, A., Haberle, R.M., Segura, T.L., Toon, O.B., Zahlne, K., 2004. The effect of impacts on the early martian climate. In: 2nd Conf. on Early Mars. Abstract 8016.

De Hon, R.A., 1992. Martian lake basins and lacustrine plains. Earth Moon Planets 56, 95–122.

Ehlmann, B.L., Mustard, J.F., Fassett, C.I., Schon, S.C., Head, J.W., Des Marais, D.J., Grant, J.A., Murchie, S.L., and the CRISM team, 2008. Clay mineralogy and organic preservation potential of lacustrine sediments from a martian delta environment, Jezero crater, Nili Fossae, Mars. Nat. Geosci. 1, 355–358.

Fassett, C.I., Head, J.W., 2005. Fluvial sedimentary deltas on Mars: Ancient deltas in a crater lake in the Nili Fossae region. Geophys. Res. Lett. 32, doi:10.1029/2005GL023456. L14201.

Fassett, C.I., Head, J.W., 2008. The timing of martian valley network activity: Constraints from buffered crater counting. Icarus 195, 61–89.

Fetter, C.W., 2001. Applied Hydrogeology, fourth ed. Prentice–Hall, Saddle River, NJ. 598 pp.

Forsythe, R.D., Zimbleman, J.R., 1995. A case for ancient evaporite basins on Mars. J. Geophys. Res. 100, 5553–5563.

Goldspiel, J.M., Squyres, S.W., 1991. Ancient aqueous sedimentation on Mars. Icarus 89, 392–410.

Grant, J.A., Parker, T.J., 2002. Drainage evolution in the Margaritifer Sinus region, Mars. J. Geophys. Res. 107, doi:10.1029/2001JE001678. 5066.

Grant, J.A., Irwin, R.P., Grotzinger, J.P., Milliken, R.E., Tornabene, L.L., McEwen, A.S., Weitz, C.M., Squyres, S.W., Glotch, T.D., Thomson, B.J., 2008. HiRISE imaging of impact megabreccia and sub-meter aqueous strata in Holden Crater, Mars. Geology 36, 195–198.

Greeley, R., Guest, J.E., 1987. Geologic map of the eastern equatorial regions of Mars. USGS Misc. Inv. Ser., Map I-1802-B.

Grimm, R.E., Harrison, K.H., 2003. A parochial view of groundwater flow on Mars. Lunar Planet. Sci. XXXIV. Abstract 2053.

Gwinner, K., Scholten, F., Jaumann, R., Roatsch, T., Oberst, J., Neukum, G., 2007. Global mapping of Mars by systematic derivation of Mars Express HRSC high-resolution digital elevation models and orthoimages. In: ISPRS IV/7 Extraterrestrial Mapping Workshop. Abstract.

Håkanson, L., 2005. The importance of lake morphometry for the structure and function of lakes. Int. Rev. Hydrobiol. 90, 433–461.

Hanna, J.C., Phillips, R.J., 2005. Hydrological modeling of the martian crust with application to the pressurization of aquifers. J. Geophys. Res. 110, doi:10.1029/2004JE002330. E01004.

Harrison, K.P., Grimm, R.E., 2005. Groundwater-controlled valley networks and the decline of surface runoff on early Mars. J. Geophys. Res. 110, doi:10.1029/2005JE002455. E12S16.

Hartmann, W.K., 2005. Martian cratering. 8. Isochron refinement and the chronology of Mars. Icarus 174, 294–320.

Hauber, E., van Gasselt, S., Chapman, M.G., Neukum, G., 2008. Geomorphic evidence for former lobate debris aprons at low latitudes on Mars: Indicators of the martian paleoclimate. J. Geophys. Res. 113, doi:10.1029/2007JE002897. E02007.

Head, J.W., Marchant, D.R., 2008. Evidence for non-polar ice deposits in the past history of Mars. Lunar Planet. Sci. XXXIX. Abstract 1295.

Head, J.W., Pratt, S., 2001. Closed chaos basins on Mars: Evidence for regional groundwater drawdown and collapse. Lunar Planet. Sci. XXXII. Abstract 1774.

Head, J.W., Kreslavsky, M.A., Pratt, S., 2002. Northern lowlands of Mars: Evidence for widespread volcanic flooding and tectonic deformation in the Hesperian Period. J. Geophys. Res. 107, doi:10.1029/2000JE001445. 5003.

Head, J.W., Carr, M.H., Russell, P.S., Fassett, C.I., 2003. Martian hydrology: The Late Noachian hydrologic cycle 7. In: Brown–Vernadsky Microsymposium 38. Abstract MS032.

Head, J.W., Marchant, D.R., Ghatan, G.J., 2004. Glacial deposits on the rim of a Hesperian–Amazonian outflow channel source trough: Mangala Valles, Mars. Geophys. Res. Lett. 31, doi:10.1029/2004GL020294. L10701.

Head, J.W., Neukum, G., Jaumann, R., Hiesinger, H., Hauber, E., Carr, M., Masson, P., Foing, B., Hoffmann, H., Kreslavsky, M., Werner, S., Milkovich, S., van Gasselt, S., the HRSC Co-Investigator Team, 2005. Tropical to mid-latitude snow and ice accumulation, flow and glaciation on Mars. Nature 434, 346–351.

Head, J.W., Wilson, L., Dickson, J., Neukum, G., 2006a. The Huygens–Hellas giant dike system on Mars: Implications for Late Noachian–Early Hesperian volcanic resurfacing and climatic evolution. Geology 34, 285–288.

Head, J.W., Marchant, D.R., Agnew, M.C., Fassett, C.I., Kreslavsky, M.A., 2006b. Extensive valley glacier deposits in the northern mid-latitudes of Mars: Evidence for Late Amazonian obliquity-driven climate change. Earth Planet. Sci. Lett. 241, 663–671.

Hiesinger, H., Head, J.W., 2002. Topography and morphology of the Argyre Basin, Mars: Implications for its geologic and hydrologic history. Planet. Space Sci. 50, 939–981.

Hiesinger, H., Head, J.W., 2004. The Syrtis Major volcanic province, Mars: Synthesis from Mars Global Surveyor data. J. Geophys. Res. (Planets) 109, doi:10.1029/2003JE002143. E01004.

Hostetler, S.W., Giorgi, F., Bates, G.T., Bartlein, P.J., 1994. Lake-atmosphere feedbacks associated with paleolakes Bonneville and Lahontan. Science 263, 665–668.

Hutchinson, G.E., 1957. A Treatise on Limnology, vol. 1, Geography, Physics, and Chemistry. Wiley & Sons, New York. 1015 pp.

Irwin, R.P., Howard, A.D., 2002. Drainage basin evolution in Noachian Terra Cimmeria, Mars. J. Geophys. Res. (Planets) 107, doi:10.1029/2001JE001818. 5056.

Irwin, R.P., Maxwell, T.A., Howard, A.D., Craddock, R.A., Leverington, D.W., 2002. A large paleolake basin at the head of Ma'adim Vallis, Mars. Science 296, 2209–2212.

Irwin, R.P., Howard, A.D., Maxwell, T.A., 2004a. Geomorphology of Ma'adim Vallis, Mars, and associated paleolake basins. J. Geophys. Res. 109, doi:10.1029/2004JE002287. E12009.

Irwin, R.P., Watters, T.R., Howard, A.D., Zimbelman, J.R., 2004b. Sedimentary resurfacing and fretted terrain development along the crustal dichotomy boundary, Aeolis Mensae, Mars. J. Geophys. Res. 109, doi:10.1029/2004JE002248. E09011.

Irwin, R.P., Howard, A.D., Craddock, R.A., Moore, J.M., 2005a. An intense terminal epoch of widespread fluvial activity on early Mars. 2. Increased runoff and paleolake development. J. Geophys. Res. (Planets) 110, doi:10.1029/2005JE002460. E12S15.

Irwin, R.P., Craddock, R.A., Howard, A.D., 2005b. Interior channels in martian valley networks: Discharge and runoff production. Geology 33, 489–492.

Irwin, R.P., Maxwell, T.A., Howard, A.D., 2007. Water budgets on early Mars: Empirical constraints from paleolake basin and watershed areas. In: 7th Int. Mars Conf. Abstract 3400.

Kramer, M.G., Potter, C.S., Des Marias, D., Peterson, D., 2003. New insights on Mars: A network of ancient lakes and discontinuous river segments. Eos Trans. AGU 84, doi:10.1029/2003EO010007.

Kreslavsky, M.A., Head, J.W., 2000. Kilometer-scale roughness of Mars: Results from MOLA data analysis. J. Geophys. Res. (Planets) 105, 26695–26711.

Lahtela, H., Korteniemi, J., Kostama, V.-P., Raitala, J., Neukum, G., and the HRSC Co-Investigator Team, 2005. The ancient lakes of the Hellas basin region as seen through the first year of Mars Express HRSC Camera. Lunar Planet. Sci. XXXVI. Abstract 1683.

Leverington, D.W., Maxwell, T.A., 2004. An igneous origin for features of a candidate crater-lake system in western Memnonia, Mars. J. Geophys. Res. (Planets) 109, doi:10.1029/2004JE002237. E06006.

Malin, M.C., Edgett, K.S., 2003. Evidence for persistent flow and aqueous sedimentation on early Mars. Science 302, 1931.

Mangold, N., Ansan, V., 2006. Detailed study of an hydrological system of valleys, a delta, and lakes in Southwest Thaumasia region, Mars. Icarus 180, 75–87.

McGill, G.E., 2000. Crustal history of north central Arabia Terra, Mars. J. Geophys. Res. (Planets) 105, 6945–6960, doi:10.1029/1999JE001175.

McGill, G.E., 2002. Geologic map transecting the highland/lowland boundary zone, Arabia Terra, Mars: Quadrangles 30332, 35332, 40332, and 45332. USGS Invest. Ser., Map I-2746, scale: 1:1M.

Moore, J.M., Howard, A., Dietrich, W.E., Schenk, P.M., 2003. Martian layered fluvial deposits: Implications for Noachian climate scenarios. Geophys. Res. Lett. 30, doi:10.1029/2003GL019002. 2292.

Mustard, J.F., Cooper, C.D., Rifkin, M.K., 2001. Evidence for recent climate changes on Mars from the identification of youthful near-surface ground ice. Nature 412, 4111–4114.

Neukum, G., Jaumann, R., and the HRSC Co-Investigator and Experiment Team, 2004. HRSC: The High Resolution Stereo Camera of Mars Express. European Space Agency Special Publication, ESA SP-1240, pp. 17–35.

Osterloo, M.M., Hamilton, V.E., Bandfield, J.L., Glotch, T.D., Baldridge, A.M., Christensen, P.R., Tornabene, L.L., Anderson, F.S., 2008. Chloride-bearing materials in the southern highlands of Mars. Science 319, 1651–1654.

Parker, T.J., Gorsline, D.S., 1991. Where is the source for Uzboi Vallis, Mars? Lunar Planet. Sci. XXII, 1033–1034.

Pieri, D.C., 1980. Martian valleys: Morphology, distributions, age, and origin. Science 210, 895–897.

Schiefer, E., Klinkenberg, B., 2004. The distribution and morphometry of lakes and reservoirs in British Columbia: A provincial inventory. Can. Geographer 48, 345–355.

Scholten, F., Gwinner, K., Roatsch, T., Matz, K.-D., Wählisch, M., Giese, B., Oberst, J., Jaumann, R., Neukum, G., and the HRSC Co-Investigator Team, 2005. Mars Express HRSC data processing—Methods and operational aspects. Photogrammetric Eng. Remote Sensing 71, 1143–1152.

Scott, D.H., Tanaka, K.L., 1986. Geologic map of the western equatorial regions of Mars. USGS Misc. Inv. Ser., Map I-1802-A.

Segura, T.L., Toon, O.B., Colaprete, A., Zahlne, K., 2002. Environmental effects of large impacts on Mars. Science 298, 1977–1980.

Smith, D.E., Zuber, M.T., Solomon, S.C., Phillips, R.J., Head, J.W., Garvin, J.B., Banerdt, W.B., Muhleman, D.O., Pettengill, G.H., Neumann, G.A., Lemoine, F.G., Abshire, J.B., Aharonson, O., Brown, C.D., Hauck, S.A., Ivanov, A.B., McGovern, P.J., Zwally, H.J., Duxbury, T.C., 1999. The global topography of Mars and implications for surface evolution. Science 284, 1495–1503.

Soderblom, L.A., Kriedler, T.J., Masursky, H., 1973. Latitudinal distribution of a debris mantle on the martian surface. J. Geophys. Res. 78, 4117–4122.

Squyres, S.W., Carr, M.H., 1986. Geomorphic evidence for the distribution of ground ice on Mars. Science 231, 249–252.

Squyres, S.W., and 49 colleagues, 2004. The Spirit Rover's Athena Science investigation at Gusev Crater, Mars. Science 305, 794–799.

Watters, T.R., 1988. Wrinkle ridge assemblages on the terrestrial planets. J. Geophys. Res. 93, 10236–10254.

Watters, T.R., 1991. Origin of periodically spaced wrinkle ridges on the Tharsis Plateau of Mars. J. Geophys. Res. 96, 15599–15616.

Watters, T.R., 2003. Lithospheric flexure and the origin of the dichotomy boundary on Mars. Geology 31, 271–274.

Watters, T.R., McGovern, P.J., 2006. Lithospheric flexure and the evolution of the dichotomy boundary on Mars. Geophys. Res. Lett. 33, doi:10.1029/2005GL024325. L08S05.

Wetzel, R.G., 2001. Limnology: Lake and River Ecosystems. Academic Press, San Diego. 1006 pp.

Winter, T.C., 1999. Relation of streams, lakes, and wetlands to groundwater flow systems. Hydrogeol. J. 7, 28–45.

Winter, T.C., Carr, M.R., 1980. Hydrologic settings of wetlands in the Cottonwood Lake area, Stutsman County, North Dakota. USGS Water Resources Inv. Rpt., pp. 80–99.